Neuropsychologia 141 (2020) 107430

Contents lists available at ScienceDirect

Neuropsychologia

journal homepage: http://www.elsevier.com/locate/neuropsychologia

Neural bases of visual processing of moving and stationary stimuli presented to the blind hemifield of hemianopic patients

Caterina A. Pedersini [a,*], Angelika Lingnau [b,c], Nicolò Cardobi [a], Javier Sanchez-Lopez [a], Silvia Savazzi [a,d,e], Carlo A. Marzi [a,e]

[a] Physiology and Psychology Section, Department of Neuroscience, Biomedicine and Movement Sciences, University of Verona, Verona, Italy
[b] Faculty of Psychology, Education and Sport Science, Institute of Psychology, University of Regensburg, Germany
[c] Centre for Mind/Brain Sciences (CIMeC), University of Trento, Trento, Italy
[d] Perception and Awareness (PandA) Laboratory, Department of Neuroscience, Biomedicine and Movement Sciences, University of Verona, Verona, Italy
[e] National Institute of Neuroscience, Verona, Italy

ARTICLE INFO

Keywords:
Hemianopia
fMRI
Visual awareness
Blindsight
Probabilistic tractography
Visual perception

ABSTRACT

Unilateral damage to post-chiasmatic visual pathways or cortical areas results in the loss of vision in the contralateral hemifield, known as hemianopia. Some patients, however, may retain the ability to perform an above chance unconscious detection or discrimination of visual stimuli presented to the blind hemifield, known as "blindsight". An important finding in blindsight research is that it can often be elicited by moving stimuli. Therefore, in the present study, we wanted to test whether moving stimuli might yield blindsight phenomena in patients with cortical lesions resulting in hemianopia, in a discrimination task where stimulus movement is orthogonal to the feature of interest. This could represent an important strategy for rehabilitation because it might improve discrimination ability of stimulus features different but related to movement, e.g. line orientation.

We tested eight hemianopic patients and eight age-matched healthy controls in an orientation discrimination task with moving or static visual stimuli. During performance of the task we carried out fMRI scanning and tractography. Behaviourally, we did not find a reliable main effect of motion on orientation discrimination; however, an important result was that in different patients blindsight could occur only with moving or stationary stimuli or with both. As to brain imaging results, following presentation of moving stimuli to the blind hemifield, a widespread fronto-parietal bilateral network was recruited including areas of the dorsal stream and in particular bilateral motion area hMT + whose activation positively correlated with behavioural performance. This bilateral network was not activated in controls suggesting that it represents a compensatory functional change following brain damage. Moreover, there was a higher activation of ipsilesional area hMT+ in patients who performed above chance in the moving condition. By contrast, in patients who performed above chance in the static condition, we found a higher activation of contralesional area V1 and extrastriate visual areas. Finally, we found a linear relationship between structural integrity of the ipsilesional pathway connecting lateral geniculate nucleus (LGN) with motion area hMT+ and both behavioural performance and ipsilesional hMT + activation. These results support the role of LGN in modulating performance as well as BOLD amplitude in the absence of visual awareness in ipsilesional area hMT+ during an orientation discrimination task with moving stimuli.

Author Contributions

CAP, AL, JSL, SS and CAM contributed to the conception and design of the study; CAP and NC contributed to the data acquisition and organization of the database; CAP and AL performed pre-processing and statistical analysis of fMRI data; NC performed pre-processing and statistical analysis of DTI data; CAP, AL and CAM wrote the first draft of the manuscript; NC wrote sections of the manuscript and created the masks of the lesions. All authors contributed to manuscript discussion, revision, and finally approval of the submitted version.

* Corresponding author. Department of Neuroscience, Biomedicine and Movement Sciences, University of Verona, Strada le Grazie, 8, 37134, Verona, Italy.
E-mail address: caterinaannalaura.pedersini@univr.it (C.A. Pedersini).

https://doi.org/10.1016/j.neuropsychologia.2020.107430
Received 22 August 2019; Received in revised form 28 February 2020; Accepted 3 March 2020
Available online 12 March 2020

1. Introduction

In the last fifty years there has been a progressive increase of interest of neuroscientists on the neural bases of awareness, a topic that was considered a sort of taboo to be left to philosophers. A major contribution to this revolutionary change has been provided by Weiskrantz and colleagues who had the great merit of following up the pioneering discovery by Pöppel et al. (1973) on four patients with acquired hemianopia or quadrantanopia as a consequence of visual cortex lesions. Despite not being able to detect brief light stimuli presented in peripheral vision in the blind hemifield, these patients could correctly saccade to them. The following year, Weiskrantz et al. (1974) in a hemianopic patient with a visual cortex lesion, not only confirmed the saccadic results of Pöppel et al. (1973) but, importantly, extended them to manual pointing which turned out to be reliably accurate despite visual stimuli being invisible. Weiskrantz named this puzzling dissociation between behaviour and perceptual awareness "blindsight". Since then the number of studies on this phenomenon has greatly increased becoming one of the most interesting approaches to understand the neural bases of visual awareness (see a recent discussion by Danckert et al., 2019). Numerous behavioural studies showed that, in forced-choice tasks, some hemianopic patients could localize, detect or discriminate the orientation of static stimuli (Weiskrantz, 1986; Morland et al., 1996), the direction of motion mainly with fast stimuli (>5°/s) (Azzopardi and Cowey, 2001; Morland et al., 1999; Barbur et al., 1980) or wavelengths (Stoerig and Cowey, 1992) (for a review see Stoerig and Cowey, 1997). Weiskrantz proposed a classification of blindsight in two sub-types: *Type I* characterized by above chance performance and a complete lack of consciousness and *Type II* characterized by above chance performance and a non-visual (or visual, see Foley and Kentridge, 2015) feeling of something occurring in the blind field. In the last few decades, it has been shown that blindsight is not merely a subcortical phenomenon as was originally hypothesized by Pöppel et al. (1973) and Weiskrantz et al. (1974). The importance of extrastriate visual areas had been highlighted previously in monkey studies (Pasik et al., 1970; Nakamura and Mishkin, 1986) and then in humans with lesion of the primary visual cortex (area V1), in terms of activation of extrastriate ipsilesional visual areas when presenting visual stimuli to the blind hemifield. In particular, a feature that has turned out to be highly relevant for yielding blindsight is visual motion, that, in absence of area V1, can activate extrastriate visual areas such as the human motion (hMT+) complex (see for review Ajina and Bridge, 2017). The human motion complex can be considered as the homologous of the motion-sensitive visual area in the middle temporal (MT) cortex plus other adjacent motion-sensitive areas (MST) of macaques (Dukelow et al., 2001). It tends to show increased activity for apparent than flicker motion (Muckli et al., 2002) as well as for horizontal or vertical component motion (Miguel Castelo-Branco, et al 2002) and is organized in columnar clusters (Schneider et al., 2019). Following visual stimulation of the blind hemifield of hemianopic patients, several studies have found a BOLD signal change of contralateral (Baseler et al., 1999; Ajina et al., 2015a; Ajina and Bridge, 2018; Papanikolaou et al., 2018) or bilateral (Goebel et al., 2001; Nelles et al., 2007; Bridge et al., 2010) area hMT+. Despite being impoverished and qualitatively different from the response of the intact contralesional area (i.e. different pattern in response to motion coherence, Ajina et al., 2015a), ipsilesional area hMT+ was clearly activated. Different studies tried to go deeper in understanding the link among behavioural performance, brain activation and level of awareness. Focusing on the role of hMT+, different authors reported a linear relation between ability to discriminate motion direction, level of awareness and activation of ipsilesional area hMT+ (Morland et al., 2004; Barbur et al., 1993; Zeki and Ffytche, 1998). Beyond hMT+, a high level of awareness has been associated with cortical activation of pre-striate and dorsolateral prefrontal cortex (Brodmann area 46), while low level of awareness has been associated with activation of subcortical structures, such as the superior colliculus, (SC) or with medial and orbital prefrontal cortical sites (Sahraie et al., 1997).

Which pathway could lead to the activation of area hMT + when V1 is damaged is still controversial. Some studies in animals and humans have provided evidence of the role of superior colliculus (SC) and pulvinar (Rodman et al., 1990; Kato et al., 2011; Kinoshita et al., 2019). Berman and Wurtz (2011), demonstrated the existence in monkeys of a pathway originating in the visual layers of the SC and projecting through the inferior pulvinar to area hMT+ and the parietal-occipital cortex. Interestingly, they showed that the directional selectivity of pulvinar neurons depended upon feedback input from hMT + rather than vice versa. At any rate, this SC-pulvinar-hMT + pathway might represent an important source of the visual properties of hMT+ in humans. Furthermore, Tamietto et al. (2010) in an hemianopic patient and in a series of studies in hemispherectomy patients with hemianopia (Leh et al., 2006; Leh et al., 2010; Georgy et al., 2016; see for review Ptito and Leh, 2007) have confirmed the role of the SC as important for various visual abilities in the absence of perceptual awareness. These studies in hemispherectomy patients are particularly relevant given that the only intact visual pathway in the operated side is represented by the retino-tectal pathway and there is no possibility of spared visual cortex. Particularly revealing is a DTI tractography study by Leh et al. (2006) in which they tested two hemispherectomy patients with blindsight and other two without. It was found that only the former showed projections from the SC on the operated side to intact contralateral and spared ipsilateral cortical areas while no cortical projections from the SC on the hemispherectomized side were present in the latter. Recently, Tran et al. (2019) have highlighted the role of this pathway in residual vision describing sub-thalamic BOLD activations in the SC and in the pulvinar in an hemianopic patient who could unconsciously perceive motion in the blind hemifield.

In contrast to the hypothesis stressing the importance of the SC input to hMT+, other studies have shown that it is the activation of the LGN (Schmid et al., 2010) as well as the integrity of structural and functional connectivity between LGN and area hMT + that ensures the presence of blindsight and represents the main characteristic to distinguish patients with and without blindsight (Bridge et al., 2008, 2010; Gaglianese et al., 2012; Ajina and Bridge, 2018).

Of course, one should also consider the possibility that both pathways are important and might provide different functional input to the hMT + complex. For example, in the monkey it has been found that the subcortical routes to MT originate in the LGN (Sincich et al., 2004), as well as in the SC through the pulvinar (Lyon et al., 2010).

In the light of this intriguing and important issue, in the present study, we used fMRI and Diffusion Tensor Imaging (DTI) techniques to shed light on the neural bases of unconscious visual motion processing in the blind hemifield of hemianopic patients. fMRI provides information on the amplitude of the BOLD signal following specific visual motion stimuli, whilst DTI allows to estimate the integrity of large-scale white matter fibres in humans by studying their microstructural properties (Catani et al., 2012; Jones et al., 2013). To do that, we studied the activation of area hMT+ during performance of an orientation discrimination task in a group of patients with long standing unilateral hemianopia sustained in adulthood and in a group of age-matched healthy controls. In this task, patients were asked to discriminate the orientation of a moving or static bar in different blocks. This enabled to investigate the modulation produced by motion on brain activity and behavioural performance during the discrimination of an orthogonal feature: orientation. Since motion has been shown to be a very effective feature for activating various cortical areas we used this paradigm for two reasons: First, to increase the probability of finding brain activation for stimulation of the blind hemifield. Second, because associating motion might be useful for possible visual rehabilitation of orientation discrimination which is a crucial feature for form perception. In addition, we investigated the integrity of white matter fibres by means of probabilistic tractography (PT) focusing on ipsilesional optic radiations (OR), LGN-hMT+ and SC-hMT + tracts. Moreover, we performed a

correlation analyses including structural measures, functional activation of hMT+, and behavioural performance. Finally, we compared differences in brain activation with behavioural performance.

2. Method

2.1. Participants

Eight hemianopic patients (3 females; mean age = 58.62 years, SD = 9.88, see Table 1), right-handed, with long-standing post-chiasmatic lesions causing visual field loss as assessed with Humphrey perimetry (see Table 1) and eight age-matched healthy participants (6 females; mean age = 60.62 years, SD = 6.69) with no history of neurological disorders were recruited. There was no significant difference between the mean age of the two groups (Wilcoxon Rank Sum Test, U=29.5 p = 0.83). Exclusion criteria included past or present neurologic disorders other than those related to hemianopia, psychiatric disorders, drugs or alcohol addiction, general cognitive impairment as revealed by a score equal or lower than 24 at the Mini Mental State Examination (Folstein et al., 1975), hemianopia diagnosed less than three months before the first testing session and presence of impairment of spatial attention (i.e. hemineglect) as tested with a neuropsychological battery including Line Bisection (Schenkenberg et al., 1980), Diller letter H cancellation (Diller et al., 1974) and Bells cancellation (Gauthier, 1989). Patients were evaluated with the Visual Function Questionnaire (VFQ25) in order to assess their subjective impressions on their visual abilities in everyday life (Mangione et al., 2001). All participants had normal or corrected-to-normal visual acuity. Informed consent was obtained after they had been fully informed about the experimental procedures and their right of quitting at any time. The study was approved by the Ethics Committee of the European Research Council and of the Azienda Ospedaliera Universitaria Integrata Verona.

2.2. Lesion details

Lesion volumes were estimated by creating lesion masks on the bias-field corrected T1-weighted image of each patient using the software ITK-SNAP (Yushkevich et al., 2006). Once created, the lesion mask was registered from the native to the standard MNI space with a spatial resolution of 1 mm, using linear transformations (FLIRT). The visualization in fsleyes (part of the FMRIB Software Library v.6.0) of each lesion mask on the T1-weighted image normalized to the standard space made it possible to localize the damaged areas. The distribution and extent of the lesion was estimated by quantifying the percentage of overlap between each lesion mask and visual areas (V1, V2, V3v, V4 and V5) extracted from the probabilistic Juelich Atlas (Eickhoff et al., 2005), after applying different thresholds to minimize overlap. No lesion affected more than 20% of the occipital lobe and there were some spared islands of primary visual cortex (V1) in all patients. In patients SL, BC and RF, the lesion affected a large portion of the ipsilesional primary visual cortex in addition to other extrastriate visual areas. In all other patients except FB, the lesion mainly involved ipsilesional extrastriate visual areas V2, V3v and V4. Area hMT+ was largely damaged in patient FB, while in patients AP and DD a smaller portion of the ipsilesional area hMT+ was affected by the lesion (see Fig. 1). Moreover, in patient FB the lesion affected the right parietal, temporal and frontal lobes (see Fig. 1S). Area hMT+ was not lesioned in any other patient.

According to the lesion site and size as well as to the type of brain damage (traumatic brain injury), we decided to exclude patient FB from the group analysis. Unlike the others, she suffered a traumatic brain injury (TBI) caused by a fall during an epileptic seizure, causing a diffuse head lesion affecting a huge portion of the right hemisphere (see Figure S1) and accompanied by behavioural symptoms going from visual to motor impairment. TBI usually causes numerous brain abnormalities such as focal shear injury, contusion, cerebral edema, vascular compromise and ventricular dilatation that can significantly affect fluid homeostasis and lead to shift, distortion and herniation of the brain (Bigler, 2001). In patient FB it was particularly difficult to differentiate between intact and damaged brain tissue as the borders of the lesion were jagged and not easily distinguishable. Moreover, right area hMT+ was functionally located within the area of encephalomacia caused by the post-traumatic haemorrhagic event, making it difficult to identify whether the BOLD signal was related to noise or to actual activation. For these reasons, we decided not to include patient FB in our analysis and to work with a more homogeneous group of 7 patients.

2.3. Experimental procedure

The experimental procedure consisted of several steps. First, patients were tested on a visual mapping paradigm outside the scanner (for further details see Sanchez-Lopez et al., 2017). This mapping, together with clinical perimetry provided by patients (see Table 1), were used to present the stimulus just in the blind area.

Next, participants were trained on the orientation discrimination task outside the scanner by using the same stimulus position as previously located with the visual mapping procedure. Controls performed the same kind of training with the stimulus in the same position of matched single patients. Finally, all participants were tested inside the fMRI scanner with the hMT + Localizer followed by the orientation discrimination task (see below). The visual stimulus was presented on a 1920 × 1080 resolution monitor with a refresh rate of 60 Hz, positioned at the back of the MRI scanner bore. Participants viewed the monitor via a double mirror mounted on the head coil. The screen subtended a visual angle of 20 × 11°. During the whole session, an MRI compatible camera was used to check for the occurrence of ocular movements. Feedback was given to patients concerning their ability to maintain fixation.

2.3.1. Human motion complex localizer

Motion-selective areas were identified by comparing the BOLD response with moving and static stimuli. The paradigm consisted of a block design with 2 runs, each lasting 350 s, one with stimuli presented in the blind and the other in the sighted hemifield. Each run was composed by 12 stimulus presentation blocks and 13 rest blocks, each lasting 14 s and started with a rest block alternated with moving and static blocks presented in a fixed order. With healthy participants, we followed the same order by presenting the stimuli in the hemifield corresponding to the blind or sighted hemifield of the matched patient in different runs. The sequence of runs was counterbalanced across participants. The stimuli were generated using Matlab 2013b (version 8.2.0.701 The MathWorks, Inc., Natick, MA, 2010) and consisted of 300 black randomly moving or static dots appearing within a circular aperture of 4° of visual angle. The background luminance was the same for all participants (17.72 cd/m^2). During the entire scanning session participants were instructed to fixate the central fixation point without giving any response.

2.3.2. Orientation discrimination task

The stimulus for the orientation discrimination task was generated using E-Prime 2.0 (Psychology Software Tools, Pittsburgh, PA) and consisted of a single black 4° × 0.5° bar horizontally (0°) or vertically (90°) oriented on a grey background of 17.72 cd/m2. The stimulus could be static or moving. In the latter case, the bar moved left-/right-ward (vertical bar) or up-/down-ward (horizontal bar) with a temporal frequency of 15°/sec, drifting 0.25° every refresh rate (16.667 ms), for 2 s, remaining within an aperture of 4° visual angle for a duration of 2 s in each trial. This kind of motion generates similar patterns of selectivity in V1 and hMT+/V5 (Hubel and Wiesel, 1968; Newsome and Paré, 1988). Moreover, different studies have demonstrated that fast visual stimuli moving at approximately 20–30°/s elicit stronger responses in hMT + than slow stimuli moving at < 6°/s (Ffytche et al., 1995; Kawakami et al., 2002; Wang et al., 2003). Those data are in keeping with either the linear relationship between amplitude of neural response in hMT+ and

Table 1
Patient's clinical description.

Patient (age/ gender)	Lesion/Visual Deficit	Perimetry (left eye/right eye)
SL (52/F)	Lesion involves the median para-sagittal portion of the left occipital lobe. Including the lingual gyrus, with peri-calcarine fissure distribution. *Visual Defect*: Right lateral homonymous hemianopia. Time elapsed between the Ischemic Stroke and the fMRI session: 92 months. 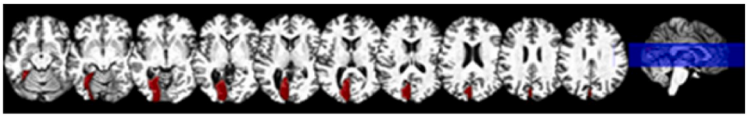	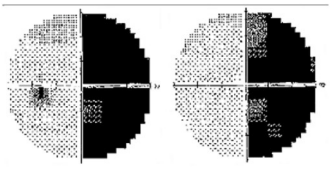
FB (53/F)	Lesion involving the right temporal, parietal and occipital lobe. In the occipital lobe, the lesion involves the superior and a portion of the middle occipital gyri with interruption of the right optic radiation. *Visual Defect*: Left lateral homonymous hemianopia. Time elapsed between the Hemorrhagic head injury and the fMRI session: 33 months. 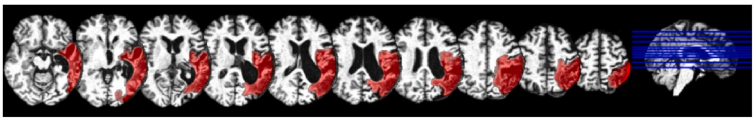	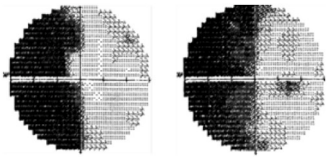
AP (50/M)	Lesion involving the inferior anterolateral portion of right occipital lobe with extension to the posterior part of temporal lobe and the upper part of right cerebellar hemisphere. Partial sparing of the Calcarine fissure. *Visual Defect*: Upper left homonymous quadrantanopia. Time elapsed between the Meningioma removal and the fMRI session: 14 months. 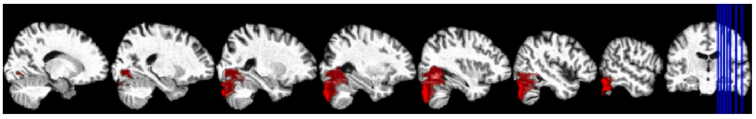	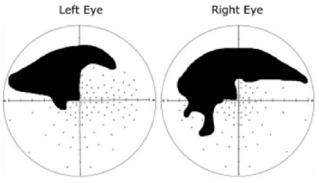
LF (54/F)	Ischemic lesion that involves the cortex of the anterior half of calcarine fissure to the origin of parieto-occipital fissure. *Visual Defect*: Upper left homonymous quadrantanopia. Time elapsed between the Ischemic Stroke and the fMRI session: 57 months. 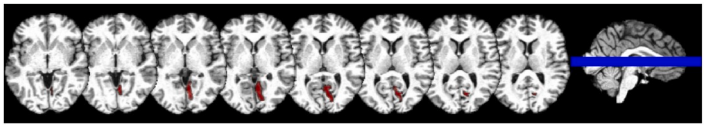	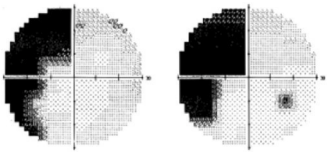
BC (71/M)	Lesion involving the medial portion of right occipital lobe, with an extension over the parieto-occipital fissure. There is an important involvement of the lingual and fusiform gyri till the occipital pole, with alterations of the Calcarine fissure. *Visual Defect*: Left lateral homonymous hemianopia. Time elapsed between the Ischemic Stroke and the fMRI session: 9 months. 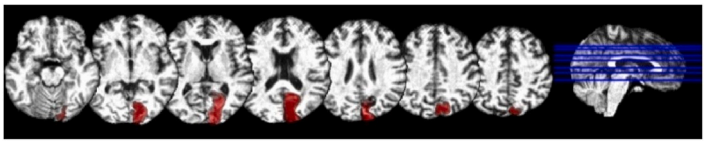	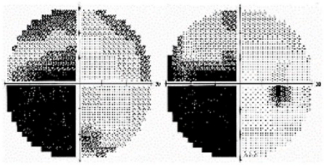
GS (77/M)	Lesion involving the antero-superior part of the right Calcarine fissure with relative sparing of the posterior part. Partial involvement of the cuneus. *Visual Defect*: Left lateral homonymous hemianopia Time elapsed between the Ischemic stroke and the fMRI session 9 months. 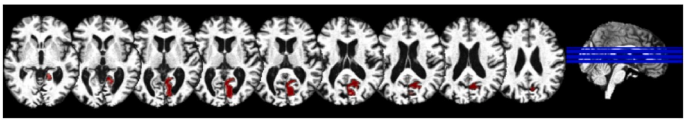	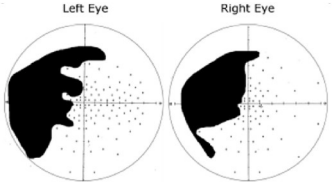
RF (54/M)	Lesion of part of the vascular territory of the left posterior cerebral artery. The alteration involves the anterior and middle portion of calcarine fissure, the lingual gyrus and the posterior part of fusiform gyrus. *Visual Defect*: Right lateral homonymous hemianopia. Time elapsed between the Ischemic Stroke and the fMRI session: 5 months. 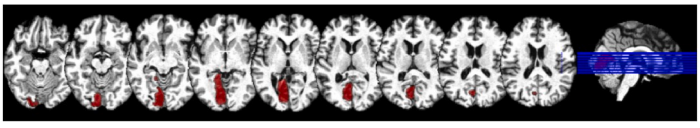	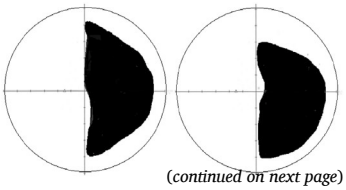

(*continued on next page*)

Table 1 (*continued*)

Patient (age/ gender)	Lesion/Visual Deficit	Perimetry (left eye/right eye)
DD (58/M)	Lesion involving the inferior-lateral part of the occipital lobe with extension to the lingual and fusiformgyri. Laterally, the lesion is below the lateral occipital sulcus. *Visual Defect*: Right lateral homonymous hemianopia. Time elapsed between the cerebral thrombosis with cortical and cerebellar occipital stroke and the fMRI session: 16 months. 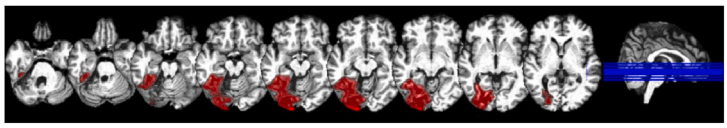	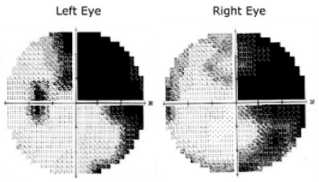

Neuroradiological description of the lesion, type of the injury, time elapsed between the lesion and the acquisition of the T1-weighted image and multi-slice representation of the T1-weighted images with the overlapped mask of the lesion. Left column: Patient's names, age and gender. Middle column: Neuroradiological description of the lesion. Right column: Humphrey monocular perimetry. Perimetries of patients SL, FB, AP, LF, BC and GS are adapted from Sanchez-Lopez et al. (2019; 2017).

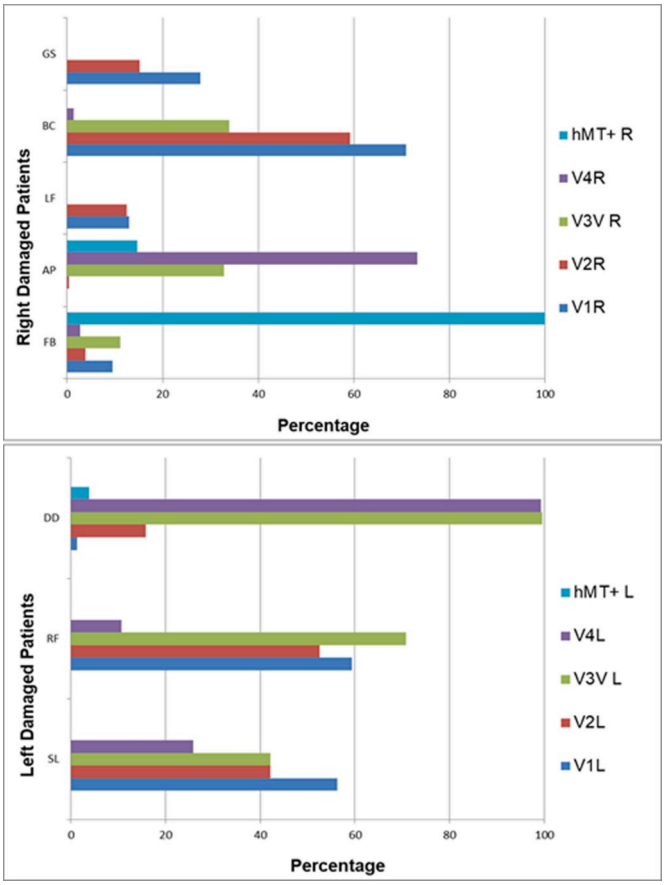

Fig. 1. Percentage of visual areas affected by the lesion in the two hemispheres (L = left; R = right).

motion speed, and the non-linear''U'' shape dependency of hMT + activation on speed (Chawla et al., 1999). Notably, contrast modulation between stimulus and background, position of the fixation point, as well as retinal eccentricity of the visual stimulus were adjusted for each patient at the beginning of the training to ensure that the stimulus was presented into the blind area and could not be consciously perceived. During the preliminary test for the best stimulus position two static bars were shown on the screen, spanning the area to be covered during the subsequent experiment by the moving or static bar. They were moved toward different directions on the screen until the blind area was found, where the patient could not see any of them. During the test for contrast, we showed a bar asking patients to respond whether they could see the stimulus or not. Every 4 trials with at least one positive response the contrast was reduced and checked until patients gave at least 4 consecutive negative responses. The resulting contrast and position were used during the training and the fMRI experiment. The same measures were used for the corresponding normally-sighted participant (see Table 2 for details).

The paradigm consisted of a block-design forced-choice orientation discrimination task in which the motion condition (moving, static) was blocked while the task-relevant orientation condition changed in each block in a pseudo-random order. The session consisted of 4 runs, each lasting 330 s. Each run consisted of 8 experimental blocks and 9 rest blocks. Within the same run the stimulus was presented in the blind or sighted quadrant in different blocks and at the beginning of each block participants were informed about the hemifield of stimulus presentation. The order of both the motion and the hemifield condition was counterbalanced across participants. Each experimental block consisted of 8 trials for a total of 64 trials presented in each hemifield for each condition. At the beginning of each trial, a black fixation point was shown and 1 s after stimulus appearance it turned red to indicate that participants should respond as fast as possible by pressing one of two MRI compatible buttons to discriminate stimulus orientation. The association between stimulus and response button was counterbalanced across participants. At the end of each block of moving or static stimuli presented in the blind hemifield patients were asked to report the average subjective level of awareness across trials by moving a line along a scale. This was to obtain information about the presence of awareness during the presentation of static or moving stimuli.

3. MRI acquisition and pre-processing

3.1. Functional data

Scanning took place in a 1.5 T Philips scanner at the Borgo Roma Hospital in Verona using a 15-channels head coil. At the beginning of the session a whole brain high-resolution (1 × 1x1 mm voxel) Ultrafast Gradient Echo 3D T1-weighted image was acquired for all patients to precisely locate the lesion and to enable co-registration of functional data with the anatomical image of each patient. Functional images were acquired covering almost the whole brain by recording from slices parallel to the bi-commissural line in the perception task and to the calcarine scissure in the hMT + localizer. 165 vol in the perception task and 190 vol in the hMT + localizer were acquired (T2*-weighted echo-planar imaging, voxel size 2 × 2x4 mm, 32 slices acquired in an ascending order, repetition time = 2000 ms, echo time = 35 ms, field of view = 230 × 230, FA = 30°) in each run and 4 dummy scans were added at the beginning of each run in order to avoid T1 saturation. Pre-

Table 2
Stimulus position and contrast for each patient.

Patient (age/gender)	Binocular Visual Mapping and stimulus position	Visual Stimulus Position and Contrast
SL (52/F)	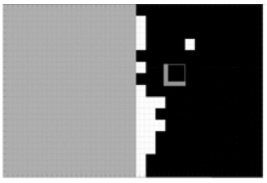	Stimulus Position: x = 5°; y = 1° Contrast: 0.5
AP (50/M)	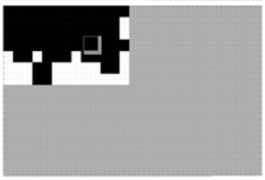	Stimulus Position: x = 5.5°; y = 5° Contrast: 0.63
LF (54/F)	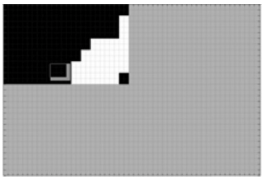	Stimulus Position: x = 12°; y = 0.5° Contrast: 0.7
BC (71/M)	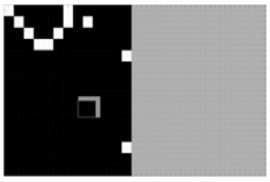	Stimulus Position: x = 6°; y = 1° Contrast: 0.7
GS (77/M)	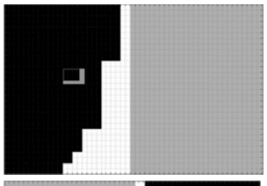	Stimulus Position: x = 9°; y = 1° Contrast: 1
RF (54/M)		Stimulus Position: x = 4°; y = 1° Contrast: 0.77
DD (58/M)	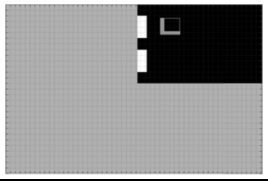	Stimulus Position: x = 5.5°; y = 9° Contrast: 0.7

Visual representation of stimulus position in the binocular visual mapping where the black area indicates the blind hemifield/quadrant, the white area indicates the residual sighted region within the blind hemifield and the grey area represents the sighted hemifield/quadrants. The stimulus is represented by two bars (one vertical and one horizontal) indicating the closest position to the fixation point. The square represents the area of visual stimulation. Left column: Patient's initials, age and gender. Middle column: representation of stimulus position in the binocular visual mapping. Right column: information on stimulus position and contrast for each patient.

processing and statistical analyses were performed using tools from FSL of FMRIB Software Library v6.0 (https://fsl.fmrib.ox.ac.uk/fsl/fslwiki/FSL) (Smith et al., 2004; Woolrich et al., 2009; Jenkinson et al., 2012). During pre-processing, non-brain tissue was extracted using BET (Brain Extraction Tool). Motion correction was performed using MCFLIRT (FMRIB Linear Image Restoration Tool with Motion Correction). Functional data were spatially smoothed using a Gaussian kernel of FWHM of 5 mm and a high-pass temporal filtering. Before performing the analysis, functional images were registered to both high-resolution structural images using FLIRT after applying BET and to a standard MNI brain template using both FLIRT and FNIRT (FMRIB Nonlinear Image Registration Tool). The same pre-processing procedure was used for both the hMT + localizer and the perception task.

3.2. DTI data pre-processing and bundles extractions

DTI analysis was conducted by means of PT with FMRIB's Diffusion Toolbox (FDT; Behrens et al., 2003, 2007). Diffusion data were pre-processed by running eddy current and motion correction (Andersson and Sotiropoulos, 2016). Bayesian Estimation of Diffusion Parameters (BEDPOSTX) was carried out on each dataset (parameters: fibres = 2, Weight = 1, Burn In = 1000). This process led to build up distributions on diffusion parameters at each voxel used to run probabilistic tractography by means of Probabilistic Tracking (PROBTRACKX) module of FDT diffusion, using a seed - target approach (parameters: number of samples = 5000, Curvature threshold = 0.2, use modified Euler streamline = on, maximum number of steps = 2000, step length = 0.5). This approach requires to define a region of interest as a seed and as a target by computing a streamline through these local samples to generate a probabilistic streamline that goes from seed to target. The regions of interest (ROIs) used as a seed were left and right LGN, left and right SC. The ROIs used as a target were left and right primary visual cortex (V1), left and right hMT+. Both LGN and V1 were extracted from the probabilistic Juelich Atlas whereas areas hMT+ were identified individually for each participant using the functional motion localizer. A mean hMT + ROI was calculated and used in probtrackx separately for each hemisphere. For the SC, binary masks were manually drawn and positioned on the anatomical 3D T1 of each patient, already registered in MNI 1 mm space. The average LGN volume was 325 mm^3, and the average SC volume was 264 mm^3. Those volumes are similar to previous reports using T1 anatomical and functional MRI scans (Kastner et al., 2004; Anderson and Rees, 2011). To automatize the process a custom modified AutoPtx script (https://fsl.fmrib.ox.ac.uk/fsl/fslwiki/AutoPtx) was applied (de Groot et al., 2013). This script allows to calculate and extract the Fractional anisotropy (FA) and Mean Diffusivity (MD) values of each bundle that are commonly used diffusion MRI indices of tissue microsctructure in presence of neuronal damage (Werring et al., 2000; Jones et al., 2013). The fibre bundles extracted were left and right LGN-V1, left and right LGN-hMT+ and left and right SC-hMT+.

4. Data analysis

4.1. Behavioural data

Reaction times (RT) faster than 150 ms from stimulus onset were considered as anticipations and not included in the statistical analyses. To assess whether performance in the blind hemifield of patients was significantly different from chance level (50%), we carried out a two-tailed binomial test on correct responses and errors for each condition and patient.

The Chi-Square Test was performed to test whether the frequency of correct/incorrect responses significantly differs from the expected frequencies by chance of the two conditions (moving/static). A contingent table was created with condition and accuracy as factors. When we extracted significant p-values, we calculated the Adjusted Residuals across rows to determine whether the frequency significantly differed from the expected count (>1.96). At group level we performed a one-sample T-test to evaluate the difference between mean accuracy and chance level separately for each condition. We performed a 2-way repeated-measure ANOVA with visual hemifield and condition as within-subject factors. Finally, we performed a correlation analysis between the behavioural performance and the level of awareness reported at the end of each block in the blind hemifield, for each condition

separately. These statistical analyses were implemented in SPSS (IBM Corp. Released 2013. IBM SPSS Statistics for Windows, Version 22.0. Armonk, NY: IBM Corp) and R version 3.6.1 (R Core Team, 2014).

4.2. Functional data

4.2.1. Regions of interest: human motion complex localizer

To localize bilateral functional areas hMT + individually in each participant, BOLD time course data were analysed by using a General Linear Model (GLM) approach with motion and static conditions as regressors. The six motion parameters of the (rigid body) realignment as well as the confound matrix of time points corrupted by large motion extracted by applying the fsl_motion_outliers tool, were included in the design matrix as additional nuisance regressors. We computed the GLM contrast moving > static dots and we masked the untresholded statistical map of each participant with the hMT + region of interest extracted from the anatomically-defined probabilistic atlas (area V5 in the Juelich Atlas) after applying a threshold of 20% to avoid visual areas overlapping. This analysis allowed to delimit borders of area hMT+ within a widespread motion-selective network extracted from the contrast of interest. The regions of interest obtained with this procedure were used in the following analyses to extract the mean activation of functional areas hMT+ in each participant during the orientation discrimination task.

4.2.2. Orientation discrimination task

For group analysis we aligned the patients' brains to a uniform pathological template following the procedure of Ajina et al., 2015a. Therefore, for patients with lesion in the left occipital lobe (n = 3) we flipped structural and functional data on the horizontal plane to make patients comparable by locating all lesions in the right hemisphere. BOLD time course data were analysed using a univariate GLM approach.

A whole brain GLM analysis was performed separately for each group with visual hemifield stimulation (blind/sighted) and motion condition (moving/static) as explanatory variables whilst age and sex were entered as nuisance regressors. Moreover, the six motion parameters of the (rigid body) realignment as well as the confound matrix of time points corrupted by large motion extracted by applying the fsl_motion_outliers tool were included in the design matrix as additional nuisance regressors. Z statistic images were created for each contrast of interest by carrying out fixed effects analyses with a cluster defining threshold ($z = 3.1$, $p < 0.001$) and the corresponding cluster probability threshold ($p = 0.05$) using Gaussian Random Field correction (Worsley et al., 1996). With a fixed-effect analysis our results reflect the data of our specific population and do not allow to make claims regarding the wider population of hemianopic patients.

The first aim of this study was the evaluation of the neural basis of visual motion perception in the sighted as well as in the blind hemifield of hemianopic patients. For this reason, we computed the whole brain fixed-effects GLM contrasts motion > baseline and motion > static, separately for each group. Next, we extracted the resulting mean parameter estimates from functionally identified areas hMT+, separately for each participant (ROI analysis). To evaluate significant differences between conditions, we computed a Wilcoxon Signed Rank Test for dependent variables on the individual parameter estimates, separately for the two groups.

Moreover, to determine whether changes in the amplitude of the BOLD signal in bilateral areas hMT + positively correlated with the behavioural performance of the group of patients, we carried out a correlation analysis (Spearman coefficient). The second aim of the study was the evaluation of the neural basis of visual processing of static stimuli in the sighted as well as in the blind hemifield. For doing that, we computed the whole brain fixed-effects contrast static > baseline, separately for each group. Then we extracted the mean parameter estimates from the ipsilesional cluster of activation within the occipital lobe, to assess the correlation between the BOLD signal change extracted and the behavioural performance in the static condition (Spearman coefficient). FDR (Benjamini and Hochberg, 1995) was applied to correct for multiple comparisons.

To test for group differences, we performed a whole brain mixed effects GLM analysis with a cluster defining threshold ($z = 2.3$, $p < 0.01$) and the corresponding probability threshold ($p = 0.05$), to create Z-statistic maps for the main contrasts of interest, entering age and gender as nuisance regressors.

Finally, we visualized levels of hMT + activation for each patient and we divided them in two subgroups based on the above-chance behavioural performance either in the moving or the static condition, to evaluate between-patients and between-subgroup differences that could reflect the modulation of behavioural performance.

All statistical maps were superimposed on a 3D volume MNI template in fsleyes to locate the brain activation obtained using the probabilistic Juelich Atlas. To visualize the statistical maps on the cortical surface, we used BrainNet Viewer (Xia et al., 2013). Statistical tests were implemented in Matlab.

4.2.3. DTI data statistical analysis

In order to assess the integrity of white matter fibres belonging to the visual system, FA and MD values were extracted from white matter tracts connecting cortex and subcortical structures of each patient and control. A comparison between values obtained from the corresponding tract in the ipsilesional and contralesional hemisphere of patients was performed by means of non-parametric Wilcoxon Test for dependent samples with each row corresponding to FA or MD values from damaged or intact hemisphere of each patient. The difference between FA and MD values obtained from corresponding tracts in patients and controls was performed by means of non-parametric Mann-Whitney test for independent samples. FDR (Benjamini and Hochberg, 1995) was applied to correct for multiple comparisons according to the number of tracts and structural measures extracted.

A measure of laterality, representing the difference in diffusivity (FA or MD) for corresponding tracts in opposite hemispheres was extracted using the formula described by Ajina et al., 2015b.

$$Laterality\ in\ patients\ (\%) = \frac{|FA/MD(intact) - FA/MD(ipsilesional)|}{FA/MD(ipsilesional)}$$

In addition, we performed a correlation analysis to assess the non-parametric Spearman correlation coefficient between structural values extracted from ipsilesional tracts and the mean activation of ipsilesional area hMT + as well as behavioural performance, with the aim of assessing the existence of a relationship between structural values, mean activation and behavioural performance.

5. Results

5.1. Behavioural performance

In the blind hemifield of hemianopic patients, mean accuracy was above 60% in either condition but above chance only in the discrimination of static stimuli, as shown by one sample *t*-test ($t = 5.05$, $p = 0.002$). Mean accuracy was analysed by using a 2×2 repeated-measures ANOVA with visual field (blind/sighted) and condition (motion/static) as within-subject factors. There was a significant main effect of visual field [$F(1,6) = 27.627$, $p < 0.002$], with higher performance in the sighted (mean = 95.08%, SD = 4.93) than the blind (mean = 63.76%, SD = 15.63) hemifield. Neither condition [$F < 1$] nor the interaction field x condition was significant [$F = 1.72$, $p > 0.238$] (see Fig. 2, left). At the end of each block with stimulus presentation to the blind hemifield, patients were asked to provide information on their average level of awareness of stimulus onset and not of stimulus orientation, On the basis of these data we calculated the awareness index, by dividing the difference by the sum of the levels of awareness reported for moving and

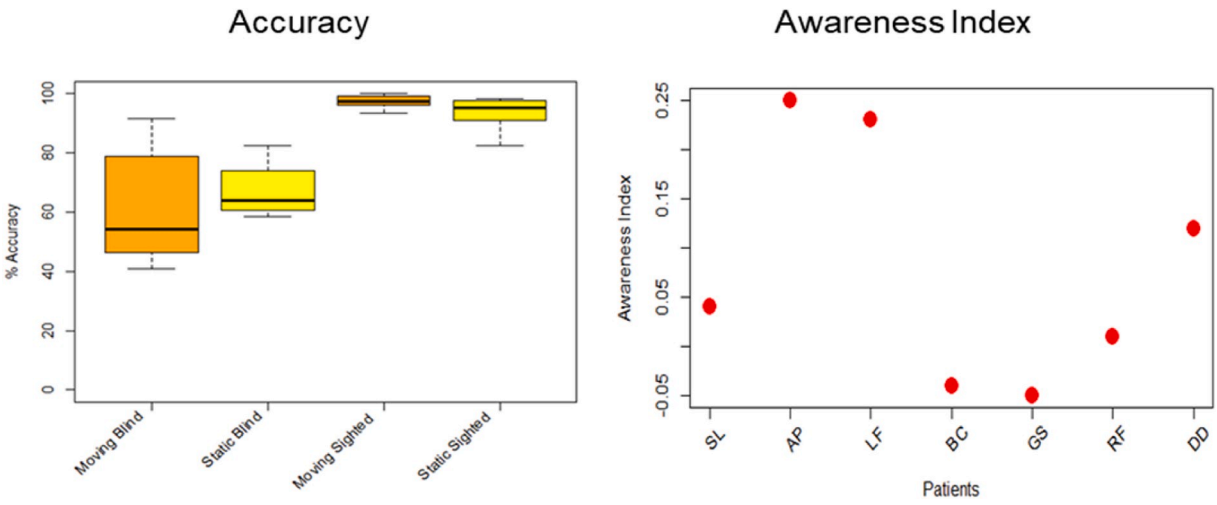

Fig. 2. Left: Boxplot showing the percentage of accuracy in discriminating the orientation of moving (orange) and stationary (yellow) stimuli following presentation to the blind and sighted hemifield of hemianopic patients. The boxplot spans the interquartile range (IQR) between the first and the third quartile; the Horizontal Line shows the median of the data; the whiskers are the two lines outside the box that extend to the highest and lowest observations [the "minimum" (Q1-1.5*IQR) and the "maximum" (Q3+1.5*IQR)]. Right: Awareness Index calculated for each patient.

static stimuli:

$$\text{Awareness Index} = \frac{(\text{AwarenessDynamic} - \text{AwarenessStatic})}{(\text{AwarenessDynamic} + \text{AwarenessStatic})}$$

with this method, a positive difference would indicate a level of awareness higher for moving compared to static stimuli and vice versa (see Table 3).

Single-subject analysis showed that 3/8 patients performed above chance in the moving condition and 4/8 in the static condition (see Table 2). According to the awareness scale, no patient was aware of the stimulus orientation, even if some patients reported to be aware of the presentation of the stimulus, mainly when it was moving (see Fig. 2, right). The two-way chi-square test showed significant results (χ^2 (1) = 11.9; p = 0.0005) only for patient LF who showed a higher number of correct responses than expected (Adjusted Residuals = 3.68). This performance was associated with visual awareness for stimulus presentation specific for the moving condition. On the contrary, patients GS and RF reported a lack of awareness for both stimulus presentation and orientation in moving and static condition with behavioural performance being significantly higher than chance only in the static condition. Finally, in patients BC and DD behavioural performance was significantly above chance in both conditions. Interestingly, they both reported to be aware of stimulus presentation with moving stimuli, whilst they reported a different level of awareness associated with the static condition: BC was aware of the stimulus presentation (this explains why the awareness index is negative) while DD reported lack of awareness.

Table 3
Behavioural performance of single patients in the blind hemifield.

PATIENT	MOVING BLIND	STATIC BLIND	AWARENESS INDEX
SL	46.03% (p = 0.615)	58.33% (p = 0.245)	0.04
AP	40.74% (p = 0.220)	60% (p = 0.203)	0.25
LF	91.2% (p < 0.001)	61.5% (p = 0.126)	0.23
BC	91.7% (p < 0.001)	77.42% (p = 0.003)	−0.04
GS	54.29% (p = 0.736)	70.73% (p = 0.012)	−0.05
RF	46.77% (p = 0.7)	63.9% (p = 0.04)	0.01
DD	66.67% (p = 0.024)	82.35% (p < 0.001)	0.12

Single patients' percentage of correct responses in the blind hemifield and corresponding results from the binomial test (only for the blind hemifield). In the last column we showed the awareness index extracted from each patient.

5.2. Functional imaging data

5.2.1. Regions of interest: human motion complex localizer

Using the mask created from the probabilistic atlas we functionally located area hMT + individually in the two groups. The median volume of area hMT+ in the damaged hemisphere was 225 ± 49 voxels (centre MNI coordinates 49.7, −66.4, 3.6), whereas was 229 ± 57 voxels (centre MNI coordinates −42, −73.6, 5.6) in the intact hemisphere. In healthy participants, the median volume of left hMT+ was 201 ± 56 voxels (centre MNI coordinates −42.3, −73.7, 5.5) and that of the right hMT+ was 214 ± 48 voxels (centre MNI coordinates 49.4, −66.7, 3.97). The size of area hMT + tended to be smaller in controls, but the distribution in the two groups did not differ significantly either when considering the ipsilesional/left hemisphere (U=38, p=0.2712, r=0.25 two-tailed) or the contralesional/right hemisphere (U=33, p=0.5979, r=0.12 two-tailed). In the following ROI analysis, we accounted for the inter-subject variability in the ROI size by bounding the hMT + to a fixed number of voxels with the highest t-values in the hMT + Localizer, corresponding to the smallest region extracted in patients (80 voxels) and controls (85 voxels). In this way, we could exclude that the results of the ROI analysis are biased by differences in ROI size.

5.2.2. Orientation discrimination task

5.2.2.1. Visual processing of moving stimuli: one-sample whole brain T-Test. To quantify the BOLD signal change in response to visual motion, the activation relative to baseline was extracted separately for patients and controls. Moreover, we measured the contrast of interest moving > static (not shown) to evaluate the activation directly related to the motion condition, removing all the confounding variables.

In **hemianopic patients** (see Fig. 3, upper left) the stimulation of the blind hemifield when compared to baseline elicited a widespread bilateral activation of visual areas V3, V4, hMT+ (main peak in ipsilesional hMT+, MNI coordinates 52, -64, 2; z = 12.4), parieto-frontal regions, as well as of the insular and premotor cortex. When considering the sighted hemifield, we observed a significant activation of

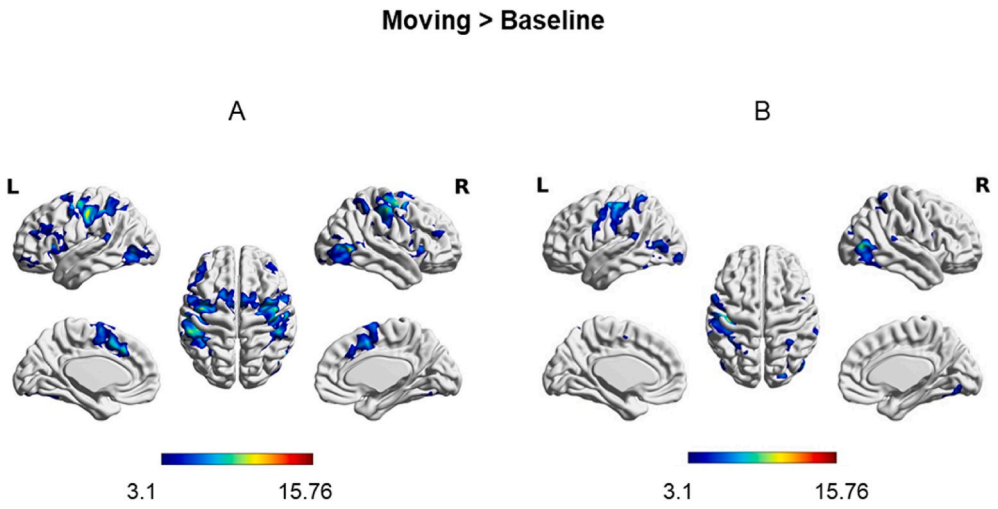

Fig. 3. Whole brain activation in patients (A) and controls (B), for the contrast of interest moving > baseline for stimulation of the blind/left hemifield. The damaged hemisphere is the right (see Methods flipping procedure). Whole brain statistical maps resulting from the GLM contrasts (fixed-effect analysis) are shown on the cortical surface and have been thresholded using Gaussian Random Field Cluster-based correction (z = 3.1, cluster probability threshold p = 0.05).

contralesional lateral occipital cortex (LOC), IPL, temporal pole and bilateral hMT+, premotor cortex, supramarginal gyrus (SMG) and parietal operculum. Moreover, the activation directly related to the motion condition (motion > static) in the blind hemifield included an extensive bilateral network composed by occipito-parieto-frontal regions, such as bilateral visual areas (V2, V3), hMT+, superior and inferior parietal lobule (SPL/IPL), ipsilesional frontal pole, contralesional motor cortex and postcentral gyrus. Instead, in the sighted hemifield, it involved a less extensive network including bilateral areas hMT+ and a small portion of left LOC and premotor cortex. These results highlight an important inter-field difference in hemianopic patients: in contrast to visual stimulation of the sighted hemifield, in the blind hemifield we found a higher activation in the moving than static condition in a widespread network involving bilateral occipital as well as ipsilesional fronto-parietal regions.

In **healthy participants** (see Fig. 3, upper right), the contrast moving > baseline in the left hemifield yielded significant activation of bilateral areas hMT+, parieto-frontal regions, as well as the right visual area V2 and LOC. The highest peak of activation (z = 11.9) was in contralateral area hMT+ (MNI coordinates: 52–76 4; no-zero voxels 227; z = 6.45). When considering the right hemifield, we observed the activation mainly of the contralateral hemisphere involving area hMT+ (MNI coordinates −52, −78, 0, z = 15.8), precentral gyrus, IPL, SMG and the premotor cortex in addition to a small activation of ipsilateral area V4 and IPL. The contrast moving > static in either left and right hemifields revealed a significant activation mainly of the occipital lobe and bilateral areas hMT+, with the main peak of activation in contralateral hMT+.

Taken together, these results confirm that the presentation of moving compared to static stimuli in the blind hemifield could elicit a much more widespread activation, involving areas beyond occipital regions. Moreover, they highlight the stronger involvement of the right premotor cortex during the discrimination of moving stimuli in both hemifields of patients in addition to the common activation of the left premotor cortex, likely due to the motor response (right hand) given at the end of each trial.

5.2.2.2. Visual processing of static stimuli: one-sample whole brain T-Test. We assessed whole brain activation following presentation of static stimuli relative to baseline separately for patients and controls.

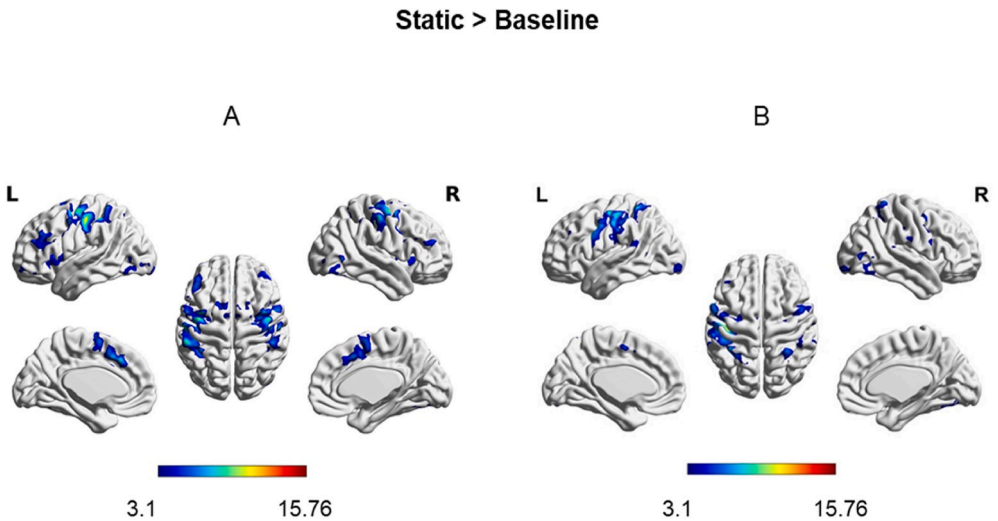

Fig. 4. Whole brain activation in patients (A) and controls (B), for the contrast of interest static > baseline for stimulation of the blind/left hemifield. The damaged hemisphere is the right (see Methods flipping procedure). Whole brain statistical maps resulting from the GLM contrasts (fixed-effect analysis) are shown on the cortical surface and have been thresholded using Gaussian Random Field Cluster-based correction (z = 3.1, cluster probability threshold p = 0.05).

In **hemianopic patients** (see Fig. 4, upper left), the contrast static > baseline when stimulating the blind hemifield yielded a significant activation of ipsilesional area hMT+ (MNI coordinates 50, -64, 0; z = 7) and bilateral premotor cortex, frontal pole and insular cortex. When considering the sighted hemifield it recruited bilateral areas hMT+ (higher involvement of the contralateral hMT+, MNI coordinates −44, −72, 2; z = 7.7), SMG and premotor cortex, contralesional LOC, V4, thalamus and ipsilesional frontal pole.

In **healthy participants**, the presentation of static stimuli in either left (see Fig. 4, upper right) and right hemifields yielded a significant activation of contralateral visual areas, hMT+, SMG, IPL and MFG as well as ipsilateral parietal regions.

The highest peak of activation was located in the left premotor cortex, likely due to the motor response that was performed with the right hand.

5.2.2.3. Two-sample unpaired T-test: patients vs controls. As to the whole brain activation following presentation of moving stimuli (Fig. 3), where we found a more widespread activation in patients than in controls, we performed a two-sample unpaired T-test to investigate whether and where brain activation significantly differed between groups. In the contrast moving > baseline, we found a larger widespread activation in patients than controls mainly involving the contralesional hemisphere and, more specifically, the left frontal pole, parietal regions and bilateral frontal orbital cortex (see Figures S2, left). In addition, when contrasting moving > static we observed a stronger recruitment of a widespread network in patients compared to controls involving the ipsilesional frontal pole, superior, middle and inferior frontal gyrus, postcentral gyrus, as well as contralesional angular and supramarginal gyrus and bilateral precentral gyrus (see Figures S2, right and S3). By contrast, no significant higher activation was found in controls compared to patients. The observed wider recruitment in patients when stimulating the blind hemifield confirms the involvement of a widespread network including other areas beyond hMT+, i.e. extrastriate visual areas, mainly in the ipsilesional hemisphere and areas belonging to the parietal and frontal lobes. By contrast, no significant difference was found in the between-group comparison when considering the sighted/right hemifield, except for a small activation of the right MTG, higher in controls than patients when contrasting moving vs baseline. Finally, we observed a stronger activation in patients for the contrast static vs baseline, involving the left frontal pole (pars triangularis); we obtained no other significant difference for the presentation of static stimuli in either the right or the left hemifield. Surprisingly, we observed a stronger activation for patients than controls when stimulating the blind hemifield with either moving or static stimuli. These results might be due to the higher cognitive effort necessary for patients to discriminate stimuli that they could not perceive.

5.2.2.4. Two-sample unpaired T-test: subgroups of patients. According to the behavioural performance (see Table 3), we divided our sample of patients in two subgroups to assess the neural bases of the difference in behavioural performance. The first subgroup was composed by those patients that showed a performance significantly higher than chance in the moving condition (LF, BC, DD); the second subgroup was composed by those with performance significantly higher than chance in the static condition (GS, RF, BC, DD). Interestingly, two of these patients (BC and DD) with higher than chance performance in both conditions reported a visual feeling of something occurring in the blind hemifield.

The contrast between the first subgroup of patients and the remaining patients (patients with performance at chance level = PT Chance Level in Figure S4) revealed a higher activation in the moving condition compared to baseline in bilateral SPL and LOC (superior division) as well as in ipsilesional fronto-parietal regions and hMT+. Looking at the whole brain activation extracted from the two subgroups separately (see Figure S4, bottom), we found that the ipsilesional area hMT+ was activated in both groups following the presentation of moving stimuli in the blind hemifield, but this activation was higher in the subgroup of patients who performed above chance in the same condition.

The mean ROI activation extracted from each patient in the moving and static condition (Fig. 5, upper left) confirmed this result, highlighting a difference going in the same direction: in the ipsilesional hMT + for stimulation of the blind hemifield, we found the highest activation in the moving condition and the biggest difference between conditions in patients LF and BC i.e. those who performed above chance in the moving condition.

Conversely, in the static > baseline contrast we observed a higher activation mainly of ipsilesional postcentral gyrus and parietal regions in the subgroup that performed above chance in the same condition. When looking at the whole brain activation extracted from the two subgroups separately, we found activation of bilateral occipital regions, mainly in contralesional visual areas V1, V2, V4, bilateral hMT+ and LOC in the subgroup that performed above chance in the static condition compared to a main bilateral fronto-parietal activation in the group of patients who performed at chance in the same condition.

The activation observed in contralesional area V1 could represent the main factor that determines the higher performance in discriminating the orientation of static stimuli. Instead, the small activation of ipsilesional area hMT + might be related to the two patients that showed a behavioural performance higher than chance in both conditions (BC and DD) (see Figure S4).

5.2.3. Orientation discrimination task: ROI analysis

To evaluate significant differences between conditions in bilateral areas hMT + functionally located for each participant, first, we extracted the mean signal amplitude per condition in each participant and then we performed a ROI analysis by comparing mean parameter estimates for moving and static condition, starting from the hypothesis of finding higher activation in the moving condition. These results provide additional information on the specificity and selectivity of hMT + activation in ipsilesional and contralesional hemispheres, despite lack of visual awareness, see Fig. 6.

In patients, we extracted higher values for moving than static stimuli from contralateral hMT+, except for patient SL (blind hemifield stimulation: Fig. 5, upper left) and patients AP and DD (sighted hemifield stimulation: Fig. 5, upper right). This result confirms the selectivity of area hMT + for moving stimuli, even in the damaged hemisphere.

The Wilcoxon-Test confirmed these results, showing a significant difference between conditions in bilateral areas hMT+ (ipsilesional z=2.41, p=0.01563, r=0.54, median moving=31.18, median static=10.55; contralesional z=2.27, p=0.02344, r=0.51, median moving=15.75, median static=9.072), when stimulating the blind hemifield, and in the contralateral hMT+ (z=2.06, p=0.03906, r=0.46, median moving=18.59, median static=10.95), when stimulating the sighted hemifield. After correcting for multiple comparisons, only the difference in bilateral areas hMT + following presentation of moving stimuli in the blind hemifield survived (FDR p=0.04688). This result highlights the great impact produced by the presentation of a moving stimulus in the blind hemifield, on the activation of bilateral areas hMT+, despite the lack of awareness (see Fig. 6, upper).

In **controls,** we extracted higher values for moving than static stimuli from contralateral hMT + when presenting stimuli in either the left or the right hemifield (see Fig. 5, lower), despite the high inter-subject variability. In this group, the Wilcoxon-Test indicates a significant difference between conditions in bilateral areas hMT+ (contralateral hMT + z=2.66, p=0.007813, r=0.59, median moving=43.95, median static=19.44; ipsilateral hMT+ z=2.42, p=0.01563, r=0.54, median moving=13.55, median static=4.288), when stimulating the left hemifield. In contrast, the presentation of moving stimuli in the right hemifield elicited higher parameter estimates in contralateral but not in ipsilateral area hMT+ (z=2.66, p=0.007813, r=0.59) with median

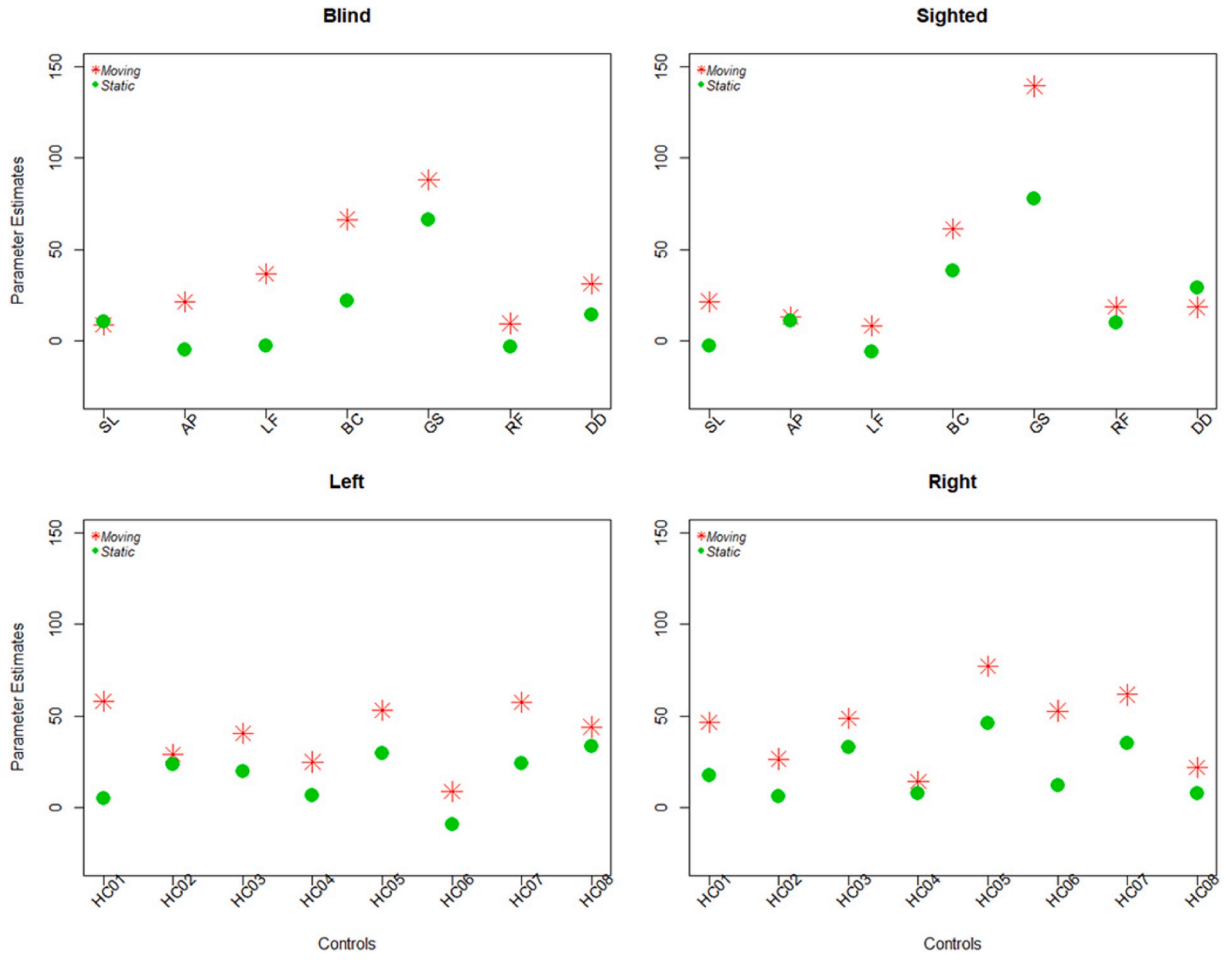

Fig. 5. Mean activation extracted from contralateral area hMT + for the contrasts of interest moving > baseline (red asterisks) and static > baseline (green dots) stimulating the blind/left and the sighted/right hemifield in patients (upper) and controls (lower). On the x-axes we show patients and controls; on the y-axes we showed mean parameter estimates extracted from hMT + for the specific contrast of interest.

values of 48.84 for the moving and 17.24 for the static condition. All the significant results survived the correction for multiple comparison (see Fig. 6, lower).

Moreover, we found that in controls as well as for the sighted hemifield of patients, the median activation of ipsilateral area hMT + following presentation of moving stimuli was smaller than that of contralateral area hMT + for static stimuli, indicating that the contralateral activation was always slightly higher that the ipsilateral activation, regardless of the nature of visual stimulation. However, a different trend was observed in patients when stimulating the blind hemifield where we found a higher activation in bilateral areas hMT+ for moving than static condition. These results suggest a selective hyper-activation for moving stimuli of the contralesional area hMT+, ipsilateral to the visual stimulation.

We carried out a correlation analysis between ROIs parameter estimates and behavioural performance. After applying a correction for multiple comparison (FDR), we found a significant positive correlation between parameter estimates extracted from contralateral area hMT+ (moving > static) and behavioural performance in the same condition (ipsilesional hMT + rho=0.86, p=0.048). In contrast, no significant correlation was observed between parameter estimates and behavioural performance in the static condition. These results confirm the positive linear relationship between hMT+ BOLD signal change and behavioural performance for moving stimuli, even though patients were not asked to discriminate motion direction.

In order to test whether activation of spared areas in V1 could be linked with the behavioural performance, we performed a correlation analysis between the activation extracted from V1 (Juelich Probabilistic Atlas with a threshold of 70%) and the behavioural performance in both conditions. We did not observe any significant correlation.

5.3. DTI results

Fig. 7 shows maximum intensity projections of white matter tracts extracted from patient AP (right lesion) and DD (left lesion), visualized on their DWI image.

Table 4 shows mean and standard deviation (sd) of FA and MD values for the three main white matter tracts. The comparison between values of FA for corresponding white matter tracts in the damaged vs. intact hemisphere showed significantly lower FA values (OR z=2.28, p=0.02249, r=0.51; LGN-hMT+z=2.29, p=0.02154, r=0.51) in the damaged compared to the intact hemisphere. A similar trend was observed for the SC-hMT+ tract but the difference was not significant (z=1.77, p=0.07593, r=0.39). No significant difference was found when comparing MD between hemispheres.

As expected, the comparison between values of FA for corresponding white matter tracts in patients and controls highlighted a significant difference between damaged hemisphere of patients and both hemispheres of controls (OR U=19, p=0.01474, r=0.54; LGN-hMT+ U=16, p=0.00823, r=0.59; SC-hMT+ U=12.5, p=0.00405, r=0.64) with lower values in the damaged hemisphere. Surprisingly, we observed a significant difference also between FA values for the contralesional LGN-hMT+ tract and either hemisphere of controls, indicating a possible structural impairment of white matter tracts in the intact hemisphere.

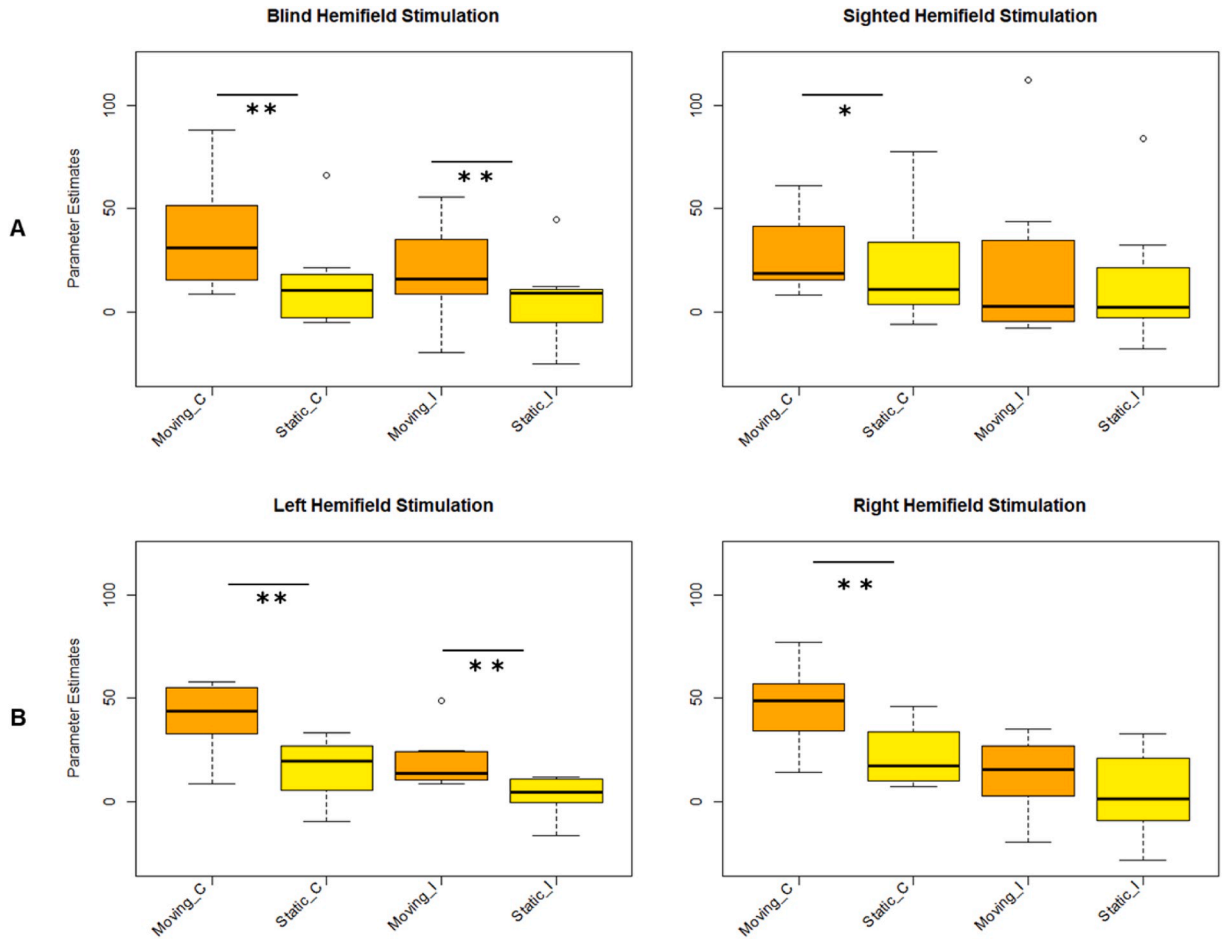

Fig. 6. Boxplot representing the within-group mean signal amplitude extracted from contralateral and ipsilateral area hMT + for the specific contrast of interest, during the stimulation of the left/blind or right/sighted visual hemifield in hemianopic patients (A) and healthy controls (B). In each panel, the x-axis shows the condition (moving or static) for the contralateral (C) or ipsilateral (I) hemisphere, and the y-axis shows the parameter estimates extracted from area hMT+. Each boxplot spans the interquartile range (IQR) between the first and the third quartile; the Horizontal Line shows the median of the data; the whiskers are the two lines outside the box that extend to the highest and lowest observations. One asterisk indicates a significant difference that does not survive FDR correction; two asterisks indicate a significant difference between conditions after applying FDR correction for multiple comparisons.

All these results survived correction for multiple comparisons (FDR). By contrast, no differences in MD survived correction for multiple comparisons. Concerning laterality, we observed a similar trend for FA and MD values. In both cases, we extracted the highest values of laterality in the OR and the lowest values in the SC-hMT+ tract. Comparing these values with those of Ajina et al., 2015b for the LGN-hMT+ tract we found that our values of FA and MD laterality are close to values they found in blindsight positive patients (FA = 13.7%, MD = 9.6%). By contrast, as expected, we observed low values of left-right laterality in controls.

5.3.1. Correlation hMT + activation-DTI measures

We obtained a significant positive correlation between the activation of ipsilesional area hMT+ in the contrast of interest moving > static and the values of FA for the ipsilesional LGN-hMT+ tract (rho=0.95, p=0.00084, FDR p=0.0025). As shown in Fig. 8 (upper panel), patient BC represents an outlier, showing the highest values of both activations in area hMT+ and FA. Importantly, results do not change when data from this patient are removed (see Fig. 8, lower left). We found a general trend of negative correlation between hMT+ activation and MD values for the same tract (rho=−0.72, p=0.068) and for the OR (rho=−0.75, p=0.066). These results indicate a positive relationship between activation of ipsilesional area hMT+ and the integrity of ipsilesional LGN-hMT+ tract, supporting the hypothesis of LGN as the main source of activation of area hMT+ in the damaged hemisphere.

We observed no significant correlation between activation of area V1 and DTI measures from all white matter tracts.

5.3.2. Correlation performance-structural measures

Importantly, we found a significant correlation between behavioural performance in the moving condition and FA (rho=0.95, p=0.00084; see Fig. 8, right) and MD (rho=−0.79, p=0.033) values for ipsilesional LGN-hMT + tract, indicating a linear relationship between the integrity of this pathway and behavioural performance (see Fig. 8, right panel). After applying correction for multiple comparison only the correlation between behavioural performance and FA values survived (FDR p=0.0025). Also in this case, BC represents an outlier with the highest values of FA and behavioural performance. Importantly, results do not change when data from this patient are removed (see Fig. 8, lower right).

The observed linear relationship between the integrity of ipsilesional LGN-hMT+ pathway, the activation of the ipsilateral area hMT+ and the behavioural performance strongly suggest this as the main source of activation of ipsilateral area hMT+. Moreover, the activation of this area positively correlates with performance confirming the functional role played in discriminative behaviour.

6. Discussion

In this study, we tested behavioural performance and brain activation during a forced-choice orientation discrimination task with moving

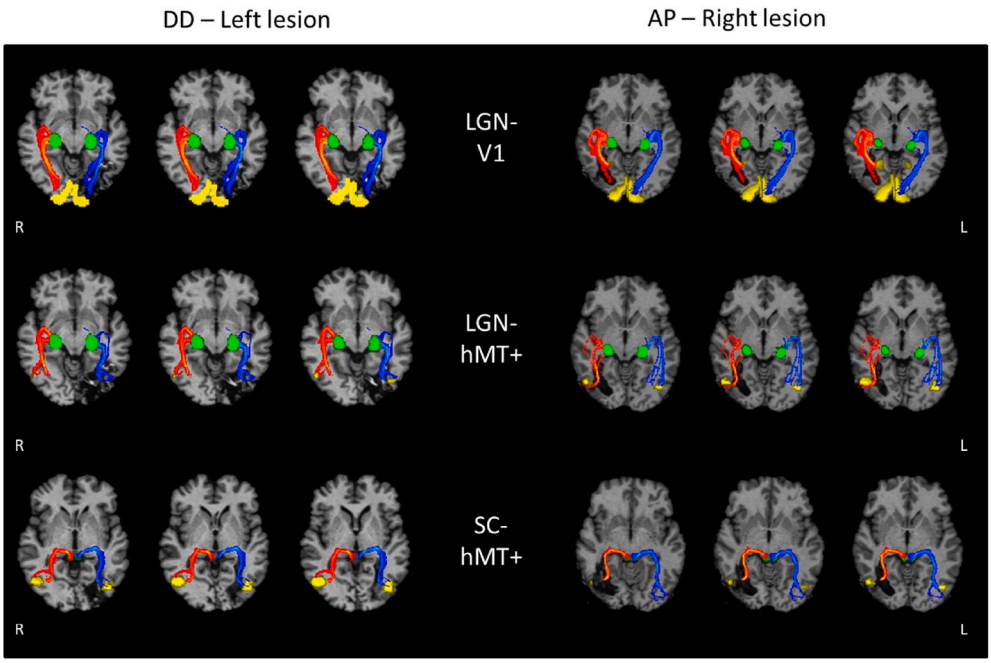

Fig. 7. Maximum intensity projections of white matter tracts extracted from patient DD (left lesion) and AP (right lesion). Green nodes indicate the seed of PT; yellow ROIs indicate the target of the probabilistic tractography. Red and blue tracts indicate right and left white matter tracts, respectively. Images are oriented according with the radiological convention (L=left hemisphere; R=right hemisphere.).

Table 4
FA and MD values extracted from white matter fibres.

FA	LGN-V1	LGN – hMT+	SC – hMT+
IPSILESIONAL	Median = 0.33 Sd = 0.12	Median = 0.3 Sd = 0.088	Median = 0.3275 Sd = 0.018
CONTRALESIONAL	Median = 0.41 Sd = 0.095	Median = 0.34 Sd = 0.10	Median = 0.35 Sd = 0.018
LATERALITY PATIENTS	17.08%	12.55%	8.39%
LEFT	Median = 0.4033 Sd = 0.034	Median = 0.39 Sd = 0.035	Median = 0.364 Sd = 0.03
RIGHT	Median = 0.42 Sd = 0.031	Median = 0.38 Sd = 0.04	Meadian = 0.3612 Sd = 0.019
LATERALITY CONTROLS	2.5%	0.5%	5%
MD	LGN-V1	LGN – hMT+	SC – hMT+
IPSILESIONAL	Median = 1.06 Sd = 0.328	Median = 0.96 Sd = 0.21	Median = 0.916 Sd = 0.06
CONTRALESIONAL	Median = 0.91 Sd = 0.19	Median = 0.87 Sd = 0.17	Median = 0.8857 Sd = 0.07
LATERALITY	15%	7%	2%
LEFT	Median = 0.91 Sd = 0.05	Median = 0.85 Sd = 0.06	Median = 0.912 Sd = 0.05
RIGHT	Median = 0.87 Sd = 0.06	Median = 0.83 Sd = 0.06	Median = 0.92 Sd = 0.06
LATERALITY CONTROLS	3.4%	3%	0.8%

or static visual stimuli presented to the blind or sighted hemifield of hemianopic patients (and healthy controls). Our study differs from previous studies in which moving dots were passively shown (Ajina et al., 2015a), or where patients were to perform a 2-AFC temporal detection task with drifting Gabor patches (Ajina et al., 2015b) or to discriminate stimulus motion direction (Benson et al., 1998; Azzopardi and Hock, 2010; Chabanat et al., 2019). Our aim was to find out whether motion could affect orientation discrimination and thus be adopted in future rehabilitation program for hemianopic patients. Various behavioural studies have demonstrated that perceptual relearning is possible following visual impairment and that can be transferred to different stimuli when performed with either moving (Huxlin, 2008), static bars (Chokron et al., 2008) or gabors (Das et al., 2014). This improvement has been associated with an increase in the activation of area hMT+ and in the kinetic occipital region (Van Oostende et al., 1997) in one hemianopic patient tested in a motion discontinuity task after training at 8 and 11 months after the occipital infarct (Vaina et al., 2014).

As mentioned in the results, at group level orientation discrimination performance did not significantly differ when presenting moving or static stimuli. Nonetheless, it is worth underlining that orientation discrimination in the blind field was significantly above chance in three out of eight patients in the moving condition and in four out of eight patients in the static condition. According to the level of awareness reported by the patients we can conclude that none of them could consciously report the stimulus feature despite some of them could report the presence of something occurring in their blind visual field. More specifically, our patients included: one with blindsight for motion (LF) associated with a feeling of something occurring in the blind hemifield, two with blindsight for static stimuli (GS, RF) with a complete lack of consciousness, two with blindsight for both stimulus conditions (BC, DD) with a weak feeling following the presentation of either static or moving stimuli (BC) or of moving stimuli (DD) and, finally, two patients with performance at chance (SL, AP). Thus, it is worth stressing the fact that blindsight can be quite variable among hemianopic patients who might show this phenomenon for one and not another stimulus feature and with or without hints of perceptual awareness. This is important both from a general and applied viewpoint. The former for relating neural mechanisms to various forms of blindsight, the latter for an experimentally based rehabilitation strategy.

The main objective of the study was to relate behavioural performance with both cortical BOLD signals assessed during the execution of the task and structural measures extracted from subcortical and cortical visual pathways. To quantify the fMRI activation of hMT+ we assessed the activation related to the moving condition following visual

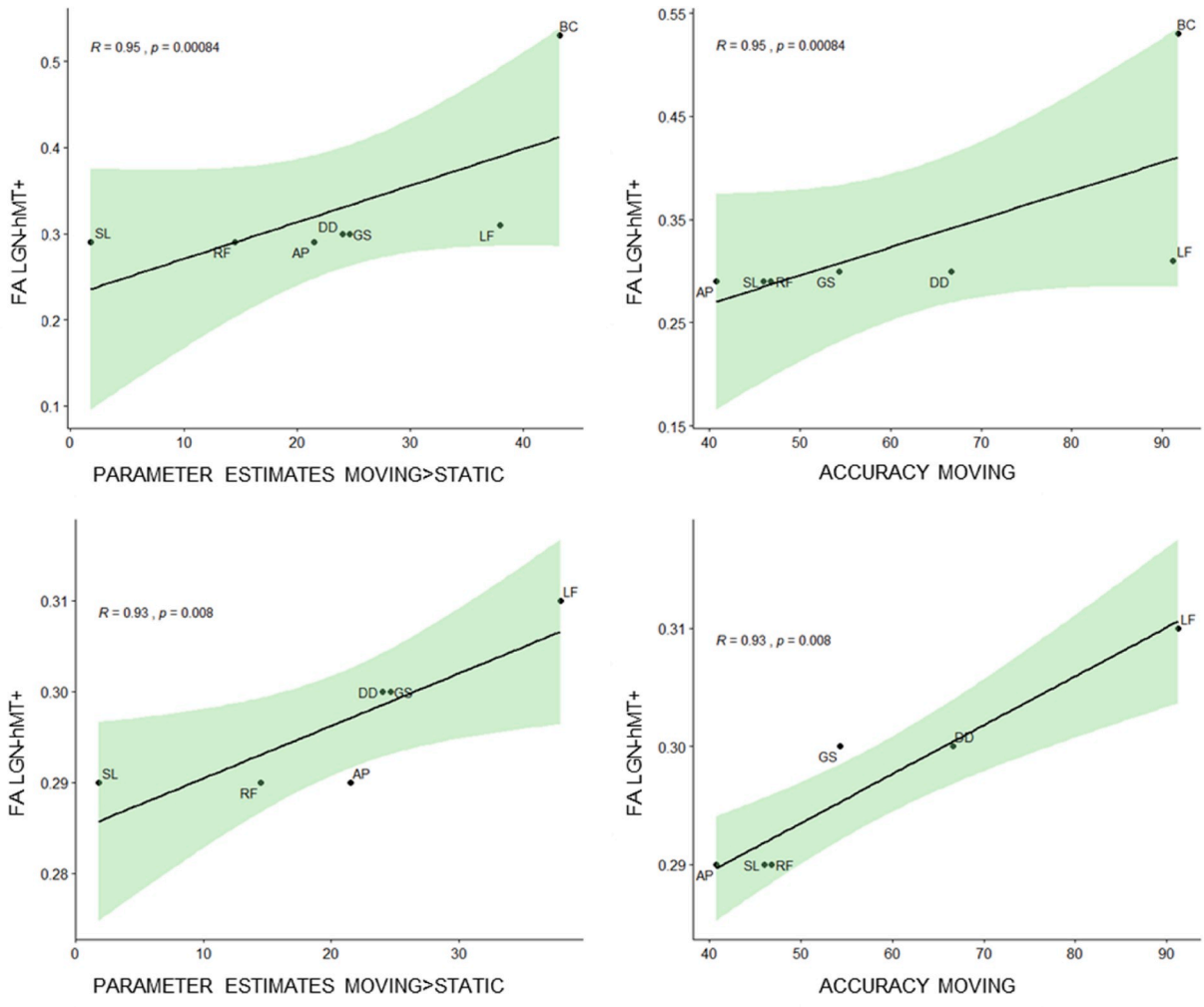

Fig. 8. Correlation between DTI measures, hMT + activation and behavioural performance. Left panel: correlation between values of FA extracted from the ipsilesional LGN-hMT+ tract and parameter estimates extracted from the ipsilesional area hMT+ in the contrast moving > static, when considering the entire group of patients (upper) and after excluding patient BC (lower). Right panel: correlation between values of FA values for the ipsilesional LGN-hMT+ tract and behavioural performance in the moving condition. Each point represents values extracted from each patient. These correlations were significant after applying FDR correction for multiple comparisons.

presentation to the blind as well the sighted hemifield of hemianopic patients and controls. In the latter, and in the sighted hemifield of patients, we found an activation of bilateral area hMT+ with a contralateral main peak, thus confirming the results of Ajina et al., 2015a. When stimulating the blind hemifield we found a similar bilateral activation of area hMT+ with an ipsilesional main peak. The bilateral activation of area hMT+ was not unexpected considering that it is composed by different motion sensitive areas including MST and FST (Tanaka et al., 2017). Moreover, it has been shown in the monkey that area MST exhibits a coarse retinotopic organization with large receptive fields extending 10° into the ipsilateral visual field (Desimone and Ungerleider, 1986; Duffy and Wurtz, 1991). A similar area which activates following stimulation of either hemifields has been described in humans (Dukelow et al., 2001; Huk et al., 2002). It is important to note that in our experiment visual stimulation was within the portion of the visual field bilaterally represented in MST. As to static stimuli, we found activation of extrastriate visual areas, more bilaterally distributed when stimulating the blind hemifield. Despite that, no significant correlation was observed between behavioural performance in the static condition and the BOLD signal change in the ipsilesional occipital cluster.

In patients, for moving stimuli presented to the blind hemifield, we found the activation of a more widespread bilateral network in comparison to controls. This network includes areas belonging to the dorsal stream, and mainly involves ipsilesional extrastriate visual areas, PPC, ventrolateral and orbital prefrontal cortex (Brodmann areas 11, 47) and a small portion of the dorsolateral prefrontal cortex (DLPFC; Brodmann area 46), i.e. a system involved in visually guided behaviour, in localizing objects in space and in motion perception (high temporal frequencies; Zavitz et al., 2017) and characterized by fast response (Norman, 2002; Tamietto and Morrone, 2016) as well as contralesional IPL, SMG and SPL. Additionally, the stronger activation of the right ventrolateral prefrontal cortex (VLPFC) belonging to the ventral attentional network could be related to the reflexive reorienting of visuo-spatial attention (Corbetta and Shulman, 2002) toward the stimulus in the blind hemifield. Finally, we observed a similar increase of functional connectivity in ipsilateral occipito-frontal connections that was stronger in patients than controls (Pedersini et al., 2020), probably related to the superior longitudinal fasciculus connecting occipital and the frontal regions and passing through the parietal lobe. The higher activation of this fronto-parietal network in patients than controls can be interpreted in the light of neural plasticity mechanisms. It has been widely demonstrated that an early V1 lesion can strengthen the pathways bypassing V1 as a consequence of neuroplastic changes (Guzzetta et al., 2010; Warner et al., 2015; Bridge et al., 2016). Our results can be interpreted as the outcome of a compensatory mechanism strengthening connections among brain regions involved in the processing of motion

(dorsal system). Besides, the importance of interhemispheric connections and the contribution of homologous regions in the intact hemisphere in hemianopic patients has been clearly demonstrated by the bilateral activation of hMT+ following blind field stimulus presentation. A bilateral activation of areas belonging to the dorsal stream has been also described by Celeghin et al. (2017) contrasting blind vs sighted field visual stimulation during testing with the Poffenberger paradigm (Poffenberger, 1912), i.e. a test of interhemispheric visuomotor transmission (for review see Marzi, 1999). Moreover, fMRI and electrophysiological studies have reported the activation of visual areas in the intact hemisphere following presentation of visual stimuli in the blind hemifield (Bittar et al., 1999; Goebel et al., 2001; Kavcic et al., 2015; Sanchez-Lopez et al., 2017). Likewise, structural studies have shown the existence in blindsight patients of crossed fibres connecting the ipsilesional with the intact hemisphere (Leh et al., 2006; Bridge et al., 2008). Finally, it has been found that following rehabilitation the intact hemisphere becomes involved in the recovery of visually evoked response from the blind field (Nelles et al., 2009).

An important result of the present study is that patients who performed above chance in the moving condition showed a higher activation of ipsilesional hMT+ with moving stimuli with respect to those who performed at chance, indicating that this specific activation can actually be related to the higher performance in the orientation discrimination of moving stimuli. Moreover, the above activation positively correlated with behavioural performance in the same condition. In parallel, we found a stronger activation of contralesional primary and extrastriate visual areas as well as ipsilesional area hMT+ in patients who performed above chance in the static condition while no occipital activation was found in those who performed at chance. These results confirm the role of ipsilesional area hMT+ in discriminating moving stimuli and highlight the importance of contralesional and ipsilesional visual areas in discriminating static stimuli presented to the blind field.

A further objective of the present study was the assessment of the integrity of fibres of three visual pathways, namely OR, LGN-hMT+ and SC-hMT+. We analysed these fibres in all patients and controls in both hemispheres and found a significant impairment of FA in all ipsilesional tracts while MD was less affected by the lesion. The LGN-hMT+ pathway was the only one that showed a significant correlation of FA with activation of ipsilesional area hMT+ and orientation discrimination in the blind hemifield. Thus, these results confirm the role of the LGN-hMT+ in both behavioural performance and activation of area hMT+ in an orientation discrimination task despite impairment of visual awareness. This is in keeping with Ajina et al., 2018 results of a retained structural and functional connectivity between ipsilesional LGN and area hMT + only in patients with blindsight.

The important role of the LGN as a source of input for visual motion processing in the blind hemifield is not necessarily in contrast with that of the SC. It is likely that both structures are important but play a different role in unconscious vision with LGN relying input related to visual feature discrimination, like the bar orientation used in the present study, while the SC might be more strictly related to stimulus detection and visuomotor tasks, see Tamietto et al. (2010).

Limitations of this study are represented first of all by the heterogeneity of our group of patients. Admittedly, the patients have somewhat different kinds of lesions affecting partly different portions of the visual pathway. Moreover, the time elapsed between the event and the fMRI scanning session was different, although always at the chronic stage.

Moreover, during the fMRI session, since we did not have access to an MR-compatible eye tracker, we could only perform visual inspection of eye movements by using an MRI compatible camera. Thus, in principle some of our data could be contaminated by spurious small saccades undetectable by visual inspection that, however, are unlikely to move the gaze to the sighted field.

Finally, due to the small sample size, when calculating the within-group mean activation, we had to perform a fixed-effect analysis. Therefore, our results reflect the data of our specific population, and therefore we cannot make claims regarding the wider population of hemianopic patients.

7. Conclusions

Following presentation of moving stimuli to the blind hemifield, despite absence of perceptual awareness, we found a significant activation of bilateral areas hMT + that positively correlated with behavioural performance in an orientation discrimination task. Unlike in controls, we found an activation of a bilateral widespread dorsal stream fronto-parietal network that presumably represents a compensatory system enabling an above chance response to unperceived moving stimuli. Furthermore, we found that the neural structures involved in above chance discrimination of static stimuli were different from those for motion stimuli and were mainly represented by contralesional striate and extrastriate visual areas and ipsilesional hMT+. This is important for rehabilitation in showing that blindsight for different stimulus features is subserved by different areas. Finally, we found that the structural measure of ipsilesional LGN-hMT+ pathway correlated with the overall ipsilesional hMT+ signal change as well as with behavioural performance. Therefore, we can conclude that in our group of hemianopic patients, this pathway is a major candidate for playing an important role for ipsilesional hMT+ activation and behavioural performance in presence of a lesion affecting the cortical visual centres and therefore the integrity of the visual field.

Acknowledgement

This work was supported by European Research Council (ERC) [Grant number 339939 “Perceptual Awareness” P.I. CAM]. The authors would like to thank Valentina Varalta, Cristina Fonte, Nicola Smania and Massimo Prior for their contribution to patients’ recruitment and clinical assessment and Giorgia Parisi for testing healthy controls.

Appendix A. Supplementary data

Supplementary data related to this article can be found at https://doi.org/10.1016/j.neuropsychologia.2020.107430.

References

Ajina, S., Bridge, H., 2017. Blindsight and unconscious vision: what they teach us about the human visual system. Neuroscientist 23, 529–541. https://doi.org/10.1177/1073858416673817.

Ajina, S., Bridge, H., 2018. Blindsight relies on a functional connection between hMT+ and the lateral geniculate nucleus, not the pulvinar. https://doi.org/10.1371/journal.pbio.2005769.

Ajina, Sara, Kennard, C., Rees, G., Bridge, H., 2015a. Motion area V5/MT+ response to global motion in the absence of V1 resembles early visual cortex. Brain 138, 164–178. https://doi.org/10.1093/brain/awu328.

Ajina, S., Pestilli, F., Rokem, A., Kennard, C., Bridge, H., 2015b. Human blindsight is mediated by an intact geniculo-extrastriate pathway. eLife 4. https://doi.org/10.7554/eLife.08935.

Anderson, E.J., Rees, G., 2011. Neural correlates of spatial orienting in the human superior colliculus. J. Neurophysiol. 106, 2273–2284. https://doi.org/10.1152/jn.00286.2011.

Andersson, J.L.R., Sotiropoulos, S.N., 2016. An integrated approach to correction for off-resonance effects and subject movement in diffusion MR imaging. Neuroimage 125, 1063–1078. https://doi.org/10.1016/j.neuroimage.2015.10.019.

Azzopardi, P., Cowey, A., 2001. Motion discrimination in cortically blind patients. Brain 124, 30–46. https://doi.org/10.1093/brain/124.1.30.

Azzopardi, P., Hock, H.S., 2010. Illusory motion perception in blindsight. Proc. Natl. Acad. Sci. Unit. States Am. 108, 876–881. https://doi.org/10.1073/pnas.1005974108.

Barbur, J.L., Ruddock, K.H., Waterfield, V.A., 1980. Human visual responses in the absence of the geniculo-calcarine projection. Brain 103, 905–928. https://doi.org/10.1093/brain/103.4.905.

Barbur, J.L., Watson, J.D.G., Frackowiak, R.S.J., Zeki, S., 1993. Conscious visual perception without VI. Brain 116, 1293–1302. https://doi.org/10.1093/brain/116.6.1293.

Baseler, H.A., Morland, A.B., Wandell, B.A., 1999. Topographic organization of human visual areas in the absence of input from the primary cortex. J. Neurosci. 19, 2619–2627. https://doi.org/10.1523/JNEUROSCI.19-07-02619.1999.
Behrens, T.E.J., Woolrich, M.W., Jenkinson, M., Johansen-Berg, H., Nunes, R.G., Clare, S., Matthews, P.M., Brady, J.M., Smith, S.M., 2003. Characterization and propagation of uncertainty in diffusion-weighted MR imaging. Magn. Reson. Med. 50, 1077–1088. https://doi.org/10.1002/mrm.10609.
Behrens, T.E.J., Berg, H.J., Jbabdi, S., Rushworth, M.F.S., Woolrich, M.W., 2007. Probabilistic diffusion tractography with multiple fibre orientations: what can we gain? Neuroimage 34, 144–155. https://doi.org/10.1016/j.neuroimage.2006.09.018.
Benjamini, Y., Hochberg, Y., 1995. Controlling the false discovery rate: a practical and powerful approach to multiple testing. J. R. Stat. Soc. Ser. B. https://doi.org/10.2307/2346101.
Benson, P.J., Guo, K., Blakemore, C., 1998. Direction discrimination of moving gratings and plaids and coherence in dot displays without primary visual cortex (V1). Eur. J. Neurosci. 10, 3767–3772. https://doi.org/10.1046/j.1460-9568.1998.00383.x.
Berman, R.A., Wurtz, R.H., 2011. Signals conveyed in the pulvinar pathway from superior colliculus to cortical area MT. J. Neurosci. 31, 373–384. https://doi.org/10.1523/JNEUROSCI.4738-10.2011.
Bigler, E.D., 2001. The lesion(s) in traumatic brain injury: implications for clinical neuropsychology. Arch. Clin. Neuropsychol. https://doi.org/10.1016/S0887-6177(00)00095-0.
Bridge, H., Thomas, O., Jbabdi, S., Cowey, A., 2008. Changes in connectivity after visual cortical brain damage underlie altered visual function. Brain 131, 1433–1444. https://doi.org/10.1093/brain/awn063.
Bittar, R.G., Ptito, M., Faubert, J., Dumoulin, S.O., Ptito, A., 1999. Activation of the remaining hemisphere following stimulation of the blind hemifield in hemispherectomized subjects. Neuroimage 10, 339–346. https://doi.org/10.1006/nimg.1999.0474.
Bridge, H., Hicks, S.L., Xie, J., Okell, T.W., Mannan, S., Alexander, I., Cowey, A., Kennard, C., 2010. Visual activation of extra-striate cortex in the absence of V1 activation. Neuropsychologia 48, 4148–4154. https://doi.org/10.1016/j.neuropsychologia.2010.10.022.
Bridge, H., Leopold, D.A., Bourne, J.A., 2016. Adaptive pulvinar circuitry supports visual cognition. Trends Cognit. Sci. 20, 146–157. https://doi.org/10.1016/j.tics.2015.10.003.
Castelo-Branco, Miguel, Formisano, Elia, Walter, Backes, Zanella, Friedhelm, Sergio Neuenschwander, W.S., R G, 2002. Birth positions in a large consultant unit. Encouraging trends. Proc. Natl. Acad. Sci. Unit. States Am. 99, 13914–13919.
Catani, M., Dell'Acqua, F., Bizzi, A., Forkel, S.J., Williams, S.C., Simmons, A., Murphy, D. G., Thiebaut de Schotten, M., 2012. Beyond cortical localization in clinico-anatomical correlation. Cortex 48, 1262–1287. https://doi.org/10.1016/J.CORTEX.2012.07.001.
Celeghin, A., Diano, M., de Gelder, B., Weiskrantz, L., Marzi, C.A., Tamietto, M., 2017. Intact hemisphere and corpus callosum compensate for visuomotor functions after early visual cortex damage. Proc. Natl. Acad. Sci. U.S.A. 114, E10475–E10483. https://doi.org/10.1073/pnas.1714801114.
Chabanat, E., Jacquin-Courtois, S., Havé, L., Kihoulou, C., Tilikete, C., Mauguière, F., Rheims, S., Rossetti, Y., 2019. Can you guess the colour of this moving object? A dissociation between colour and motion in blindsight. Neuropsychologia 128, 204–208. https://doi.org/10.1016/j.neuropsychologia.2018.08.006.
Chawla, D., Buechel, C., Edwards, R., Howseman, A., Josephs, O., Ashburner, J., Friston, K.J., 1999. Speed-dependent responses in V5: a replication study. Neuroimage 9, 508–515. https://doi.org/10.1006/nimg.1999.0432.
Chokron, S., Perez, C., Obadia, M., Gaudry, I., Laloum, L., Gout, O., 2008. From blindsight to sight: cognitive rehabilitation of visual field defects. Restor. Neurol. Neurosci. 26, 305–320.
Corbetta, M., Shulman, G.L., 2002. Control of goal-directed and stimulus-driven attention in the brain. Nat. Rev. Neurosci. 3, 201–215. https://doi.org/10.1038/nrn755.
Danckert, J., Tamietto, M., Rossetti, Y., 2019. Blindsight. Cortex. https://doi.org/10.1016/J.CORTEX.2019.01.027.
Das, A., Tadin, D., Huxlin, K.R., 2014. Beyond blindsight: properties of visual relearning in cortically blind fields. J. Neurosci. 34, 11652–11664. https://doi.org/10.1523/JNEUROSCI.1076-14.2014.
de Groot, M., Vernooij, M.W., Klein, S., Ikram, M.A., Vos, F.M., Smith, S.M., Niessen, W. J., Andersson, J.L.R., 2013. Improving alignment in Tract-based spatial statistics: evaluation and optimization of image registration. Neuroimage 76, 400–411. https://doi.org/10.1016/j.neuroimage.2013.03.015.
Desimone, R., Ungerleider, L.G., 1986. Multiple visual areas in the caudal superior temporal sulcus of the macaque. J. Comp. Neurol. 248, 164–189. https://doi.org/10.1002/cne.902480203.
Diller, L., Ben-Yishay, Y., Gerstman, L.J., Goodkin, R., Gordon, W., Weinberg, J., Mandleberg, I., Schulman, P., Shah, N., 1974. Studies in Cognition and Rehabilitation in Hemiplegia.
Duffy, C.J., Wurtz, R.H., 1991. Sensitivity of MST neurons to optic flow stimuli. II. Mechanisms of response selectivity revealed by small-field stimuli. J. Neurophys. 65 (6), 1346–1359. https://doi.org/10.1152/jn.1991.65.6.1346.
Dukelow, S.P., X Desouza, J.F., Culham, J.C., Van Den Berg, A.V., Menon, R.S., Vilis, T., X DeSouza, J.F., van den Berg, A.V., Vilis Distinguishing subregions, T., 2001. Distinguishing Subregions of the Human MT+ Complex Using Visual Field and Pursuit Eye Movements.
Eickhoff, S.B., Stephan, K.E., Mohlberg, H., Grefkes, C., Fink, G.R., Amunts, K., Zilles, K., 2005. A new SPM toolbox for combining probabilistic cytoarchitectonic maps and functional imaging data. Neuroimage 25, 1325–1335. https://doi.org/10.1016/j.neuroimage.2004.12.034.
Ffytche, D.H., Guy, C.N., Zeki, S., 1995. The parallel visual motion inputs into areas VI and V5 of human cerebral cortex. Brain 118, 1375–1394.
Foley, R., Kentridge, R.W., 2015. Type-2 blindsight: empirical and philosophical perspectives. Conscious. Cognit. 32, 1–5. https://doi.org/10.1016/j.concog.2015.01.008.
Folstein, M.F., Folstein, S.E., McHugh, P.R., 1975. "Mini-mental state": a practical method for grading the cognitive state of patients for the clinician. J. Psychiatr. Res. 12, 189–198. https://doi.org/10.1016/0022-3956(75)90026-6.
Gaglianese, A., Costagli, M., Bernardi, G., Ricciardi, E., Pietrini, P., 2012. Evidence of a direct influence between the thalamus and hMT+ independent of V1 in the human brain as measured by fMRI. Neuroimage 60, 1440–1447. https://doi.org/10.1016/j.neuroimage.2012.01.093.
Gauthier, L., 1989. The Bells Testt : a quantitative and qualitative test for visual neglect. Int. J. Clin. Neuropsychol. 11, 49–54.
Georgy, L., Celeghin, A., Marzi, C.A., Tamietto, M., Ptito, A., 2016. The superior colliculus is sensitive to gestalt-like stimulus configuration in hemispherectomy patients. Cortex 81, 151–161. https://doi.org/10.1016/j.cortex.2016.04.018.
Goebel, R., Muckli, L., Zanella, F.E., Singer, W., Stoerig, P., 2001. Sustained extrastriate cortical activation without visual awareness revealed by fMRI studies of hemianopic patients. Vision Res 41, 1459–1474. https://doi.org/10.1016/S0042-6989(01)00069-4.
Guzzetta, A., D'acunto, G., Rose, S., Tinelli, F., Boyd, R., Cioni, G., 2010. Plasticity of the visual system after early brain damage. Dev. Med. Child Neurol. https://doi.org/10.1111/j.1469-8749.2010.03710.x.
Hubel, D.H., Wiesel, T.N., 1968. Receptive fields and functional architecture of monkey striate cortex. J. Physiol. 195, 215–243.
Huk, A.C., Dougherty, R.F., Heeger, D.J., 2002. Retinotopy and functional subdivision of human areas MT and MST. J. Neurosci. 22, 7195–7205 doi:20026661.
Huxlin, K.R., 2008. Perceptual plasticity in damaged adult visual systems. Vision Res 48, 2154–2166. https://doi.org/10.1016/j.visres.2008.05.022.
Jenkinson, M., Beckmann, C.F., Behrens, T.E.J., Woolrich, M.W., Smith, S.M., 2012. FSL. Neuroimage 62, 782–790. https://doi.org/10.1016/j.neuroimage.2011.09.015.
Jones, D.K., Knösche, T.R., Turner, R., 2013. Comments and Controversies White matter integrity, fiber count, and other fallacies: the do's and don'ts of diffusion MRI. Neuroimage 73, 239–254. https://doi.org/10.1016/j.neuroimage.2012.06.081.
Kastner, S., O'Connor, D.H., Fukui, M.M., Fehd, H.M., Herwig, U., Pinsk, M.A., 2004. Functional imaging of the human lateral geniculate nucleus and pulvinar. J. Neurophysiol. 91, 438–448. https://doi.org/10.1152/jn.00553.2003.
Kato, R., Takaura, K., Ikeda, T., Yoshida, M., Isa, T., 2011. Contribution of the retino-tectal pathway to visually guided saccades after lesion of the primary visual cortex in monkeys. Eur. J. Neurosci. 33, 1952–1960. https://doi.org/10.1111/j.1460-9568.2011.07729.x.
Kavcic, V., Triplett, R.L., Das, A., Martin, T., Huxlin, K.R., 2015. Role of inter-hemispheric transfer in generating visual evoked potentials in V1-damaged brain hemispheres. Neuropsychologia 68, 82–93. https://doi.org/10.1016/j.neuropsychologia.2015.01.003.
Kawakami, O., Kaneoke, Y., Maruyama, K., Kakigi, R., Okada, T., Sadato, N., Yonekura, Y., 2002. Visual detection of motion speed in humans: spatiotemporal analysis by fMRI and MEG. Hum. Brain Mapp. 16, 104–118. https://doi.org/10.1002/hbm.10033.
Kinoshita, M., Kato, R., Isa, K., Kobayashi, K., 2019. Dissecting the circuit for blindsight ; critical role of the pulvinar. Nat. Commun. 1–24. https://doi.org/10.1038/s41467-018-08058-0.
Leh, S.E., Johansen-Berg, H., Ptito, A., 2006. Unconscious vision: new insights into the neuronal correlate of blindsight using diffusion tractography. Brain 129, 1822–1832. https://doi.org/10.1093/brain/awl111.
Leh, S.E., Ptito, A., Schönwiesner, M., Chakravarty, M.M., Mullen, K.T., 2010. Blindsight mediated by an S-Cone-independent collicular pathway: an fMRI study in hemispherectomized subjects. J. Cognit. Neurosci. 22, 670–682. https://doi.org/10.1162/jocn.2009.21217.
Lyon, D.C., Nassi, J.J., Callaway, E.M., 2010. A disynaptic relay from superior colliculus to dorsal stream visual cortex in macaque. Monkey 65, 270–279. https://doi.org/10.1016/j.neuron.2010.01.003.
Mangione, C.M., Lee, P.P., Gutierrez, P.R., Spritzer, K., Berry, S., Hays, R.D., National Eye Institute Visual Function Questionnaire Field Test Investigators, 2001. Development of the 25-item national eye institute visual function Questionnaire. Arch. Ophthalmol. (Chicago, Ill. 1960 119, 1050–1058.
Marzi, C.A., 1999. The Poffenberger paradigm: a first, simple, behavioural tool to study interhemispheric transmission in humans. Brain Res. Bull. 50, 421–422. https://doi.org/10.1016/S0361-9230(99)00174-4.
Morland, A.B., Ogilvie, J.A., Ruddock, K.H., W J R, 1996. Orientation discrimination is im paired in the absence of the striate cortical contribution to hum an vision. Proc. Roy. Soc. Lond. 263, 633–640.
Morland, a B., Jones, S.R., Finlay, a L., Deyzac, E., Le, S., Kemp, S., 1999. Visual-perception of motion, luminance and color in a human hemianope. Brain 122, 1183–1198.
Morland, A.B., Lê, S., Carroll, E., Hoffmann, M.B., Pambakian, A., 2004. The role of spared calcarine cortex and lateral occipital cortex in the responses of human hemianopes to visual motion. J. Cognit. Neurosci. 16, 204–218. https://doi.org/10.1162/089892904322984517.
Muckli, L., Kriegeskorte, N., Lanfermann, H., Zanella, F.E., Singer, W., Goebel, R., 2002. Apparent motion: event-related functional magnetic resonance imaging of perceptual switches and States. J. Neurosci. 22, 1–5. https://doi.org/10.1523/jneurosci.22-09-j0003.2002.

Nakamura, R.K., Mishkin, M., 1986. Chronic 'blindness' following lesions of nonvisual cortex in the monkey. Exp. Brain Res. 63, 173–184. https://doi.org/10.1007/BF00235661.
Nelles, G., de Greiff, A., Pscherer, A., Forsting, M., Gerhard, H., Esser, J., Diener, H.C., 2007. Cortical activation in hemianopia after stroke. Neurosci. Lett. 426, 34–38. https://doi.org/10.1016/j.neulet.2007.08.028.
Nelles, G., Pscherer, A., de Greiff, A., Forsting, M., Gerhard, H., Esser, J., Diener, H.C., 2009. Eye-movement training-induced plasticity in patients with post-stroke hemianopia. J. Neurol. 256, 726–733. https://doi.org/10.1007/s00415-009-5005-x.
Newsome, W.T., Paré, E.B., 1988. A selective impairment of motion perception following lesions of the middle temporal visual area (MT). J. Neurosci. 8, 2201–2211. https://doi.org/10.1523/JNEUROSCI.08-06-02201.1988.
Norman, J., 2002. Two visual systems and two theories of perception: an attempt to reconcile the constructivist and ecological approaches. Behav. Brain Sci. 25, 73–96. https://doi.org/10.1017/S0140525X0200002X.
Papanikolaou, A., Keliris, G.A., Papageorgiou, T.D., Schiefer, U., Logothetis, N.K., Smirnakis, S.M., 2018. Organization of area hV5/MT+ in subjects with homonymous visual field defects. Neuroimage. https://doi.org/10.1016/j.neuroimage.2018.03.062.
Pasik, T., Pasik, P., Valciukas, J.A., 1970. Nystagmus induced by stationary repetitive light flashes in monkeys. Brain Res. 19, 313–317. https://doi.org/10.1016/0006-8993(70)90446-4.
Pedersini, C.A., Guardia-Olmos, J., Montala-Flaquer, M., Cardobi, N., Sanchez-Lopez, J., Parisi, G., Savazzi, S., Marzi, C.A., 2020. Functional interactions in patients with hemianopia: a graph theory-based connectivity study of resting fMRI signal. PloS One. https://doi.org/10.1371/journal.pone.0226816.
Poffenberger, A.T., 1912. Reaction Time to Retinal Stimulation, with | Hathi Trust Digital Library [WWW Document]. Sci. Press, New York accessed 4.18.19. https://catalog.hathitrust.org/Record/001633246.
Pöppel, E., Held, R., Frost, D., 1973. Residual visual function after brain wounds involving the central visual pathways in man. Nature 243, 295–296. https://doi.org/10.1038/243295a0.
Ptito, A., Leh, S.E., 2007. Neural substrates of blindsight after hemispherectomy. Neuroscientist 13, 506–518. https://doi.org/10.1177/1073858407300598.
R Core Team, 2014. R: the R Project for Statistical Computing [WWW Document]. URL. https://www.r-project.org/.
Rodman, H.R., Gross, C.G., Albrightb, T.D., 1990. Afferent basis of visual response properties in area MT of the macaque. II. Effects of superior colliculus removal. J. Neurosci. 10 (4), 1154–1164.
Sahraie, A., Weiskrantz, L., Barbur, J.L., Simmons, A.S., Williams, S.C.R., Brammer, M.J., 1997. Pattern of neuronal activity associated with conscious and. Proc. Natl. Acad. Sci. U.S.A. 94, 9406–9411.
Sanchez-Lopez, J., Pedersini, C.A., Di Russo, F., Cardobi, N., Fonte, C., Varalta, V., Prior, M., Smania, N., Savazzi, S., Marzi, C.A., 2017. Visually evoked responses from the blind field of hemianopic patients. Neuropsychologia. https://doi.org/10.1016/j.neuropsychologia.2017.10.008.
Sanchez-Lopez, J., Savazzi, S., Pedersini, C.A., Cardobi, N., Marzi, C.A., 2019. Neural correlates of visuospatial attention to unseen stimuli in hemianopic patients. A steady-state visual evoked potential study. Front. Psychol. 10, 198. https://doi.org/10.3389/fpsyg.2019.00198.
Schenkenberg, T., Bradford, D.C., Ajax, E.T., 1980. Line bisection and unilateral visual neglect in patients with neurologic impairment. Neurology 30. https://doi.org/10.1212/WNL.30.5.509, 509–509.
Schmid, M.C., Mrowka, S.W., Turchi, J., Saunders, R.C., Wilke, M., Peters, A.J., Ye, F.Q., Leopold, D.A., 2010. Blindsight depends on the lateral geniculate nucleus. Nature 466, 373–377. https://doi.org/10.1038/nature09179.
Schneider, M., Kemper, V.G., Emmerling, T.C., De Martino, F., Goebel, R., 2019. Columnar clusters in the human motion complex reflect consciously perceived motion axis. Proc. Natl. Acad. Sci. Unit. States Am. 116, 5096–5101. https://doi.org/10.1073/pnas.1814504116.
Sincich, L.C., Park, K.F., Wohlgemuth, M.J., Horton, J.C., 2004. Bypassing V1: a direct geniculate input to area MT. Nat. Neurosci. 7, 1123–1128. https://doi.org/10.1038/nn1318.
Smith, S.M., Jenkinson, M., Woolrich, M.W., Beckmann, C.F., Behrens, T.E.J., Johansen-Berg, H., Bannister, P.R., De Luca, M., Drobnjak, I., Flitney, D.E., Niazy, R.K., Saunders, J., Vickers, J., Zhang, Y., De Stefano, N., Brady, J.M., Matthews, P.M., 2004. Advances in functional and structural MR image analysis and implementation as FSL. Neuroimage 23, S208–S219. https://doi.org/10.1016/j.neuroimage.2004.07.051.
Stoerig, P., Cowey, A., 1992. Wavelength discrimination in blindsight. Brain 115, 425–444. https://doi.org/10.1093/brain/115.2.425.
Stoerig, P., Cowey, A., 1997. Blindsight in man and monkey. Brain 120, 535–559. https://doi.org/10.1093/brain/120.3.535.
Tamietto, M., Morrone, M.C., 2016. Visual plasticity: blindsight bridges anatomy and function in the visual system. Curr. Biol. 26, R70–R73. https://doi.org/10.1016/j.cub.2015.11.026.
Tamietto, M., Cauda, F., Corazzini, L.L., Savazzi, S., Marzi, C.A., Goebel, R., Weiskrantz, L., de Gelder, B., 2010. Collicular vision guides nonconscious behavior. J. Cognit. Neurosci. 22, 888–902. https://doi.org/10.1162/jocn.2009.21225.
Tanaka, K., Sugita, Y., Moriya, M., Saito, H., 2017. Analysis of object motion in the ventral part of the medial superior temporal area of the macaque visual cortex. J. Neurophysiol. 69, 128–142. https://doi.org/10.1152/jn.1993.69.1.128.
Tran, A., MacLean, M.W., Hadid, V., Lazzouni, L., Nguyen, D.K., Tremblay, J., Dehaes, M., Lepore, F., 2019. Neuronal mechanisms of motion detection underlying blindsight assessed by functional magnetic resonance imaging (fMRI). Neuropsychologia. https://doi.org/10.1016/j.neuropsychologia.2019.02.012.
Vaina, L.M., Soloviev, S., Calabro, F.J., Buonanno, F., Passingham, R., Cowey, A., 2014. Reorganization of retinotopic maps after occipital lobe infarction. J. Cognit. Neurosci. 26, 1266–1282. https://doi.org/10.1162/jocn_a_00538.
Van Oostende, S., Sunaert, S., Van Hecke, P., Marchal, G., Orban, G.A., 1997. The kinetic occipital (KO) region in man: an fMRI study. Cerebr. Cortex 7, 690–701. https://doi.org/10.1093/cercor/7.7.690.
Wang, L., Kaneoke, Y., Kakigi, R., 2003. Spatiotemporal separability in the human cortical response to visual motion speed: a magnetoencephalography study. Neurosci. Res. 47, 109–116. https://doi.org/10.1016/S0168-0102(03)00191-3.
Warner, C.E., Kwan, W.C., Wright, D., Johnston, L.A., Egan, G.F., Bourne, J.A., 2015. Preservation of vision by the pulvinar following early-life primary visual cortex lesions. Curr. Biol. 25, 424–434. https://doi.org/10.1016/J.CUB.2014.12.028.
Weiskrantz, L., 1986. Blindsight: A Case Study and Implications.
Weiskrantz, L., Warrington, E.K., Sanders, M.D., Marshall, J., 1974. Visual capacity in the hemianopic field following a restricted occipital ablation. Brain 97, 709–728. https://doi.org/10.1093/brain/97.4.709.
Werring, D.J., Toosy, A.T., Clark, C.A., Parker, G.J., Barker, G.J., Miller, D.H., Thompson, A.J., 2000. Diffusion tensor imaging can detect and quantify corticospinal tract degeneration after stroke. J. Neurol. Neurosurg. Psychiatry 69, 269–272.
Woolrich, M.W., Jbabdi, S., Patenaude, B., Chappell, M., Makni, S., Behrens, T., Beckmann, C., Jenkinson, M., Smith, S.M., 2009. Bayesian analysis of neuroimaging data in FSL. Neuroimage 45, S173–S186. https://doi.org/10.1016/j.neuroimage.2008.10.055.
Worsley, K.J., Marrett, S., Neelin, P., Vandal, A.C., Friston, L.J., E A C, 1996. A unified statistical approach for determining significant signals in location and scale space images of cerebral activation. Quantification of Brain Function Using PET, pp. 327–333. https://doi.org/10.1016/b978-012389760-2/50066-9.
Xia, M., Wang, J., He, Y., 2013. BrainNet viewer: a network visualization tool for human brain connectomics. PloS One 8. https://doi.org/10.1371/journal.pone.0068910.
Yushkevich, P.A., Piven, J., Hazlett, H.C., Smith, R.G., Ho, S., Gee, J.C., Gerig, G., 2006. User-guided 3D active contour segmentation of anatomical structures: significantly improved efficiency and reliability. Neuroimage 31, 1116–1128. https://doi.org/10.1016/j.neuroimage.2006.01.015.
Zavitz, E., Rosa, M.G.P., Price, N.S.C., 2017. Primate visual cortex. Ref. Modul. Neurosci. Biobehav. Psychol. https://doi.org/10.1016/B978-0-12-809324-5.03196-5.
Zeki, S., Ffytche, D.H., 1998. The Riddoch syndrome: insights into the neurobiology of conscious vision. Brain 121, 25–45. https://doi.org/10.1093/brain/121.1.25.